

FAX: +44 (0) 191-334-9104

email: martin.schroeder@durham.ac.uk

22 **Running Title:** Bypass of phosphorylation in activation of Ire1

23 **Keywords:** endoplasmic reticulum, Ire1, unfolded protein response, phosphorylation, protein

24 kinase, phosphorylation-independent RD kinase, stress response

25 **Word count for the Materials and Methods section:** 3,149

26 **Combined word count for the Introduction, Results, and Discussion sections:** 5,340

27

28 **Abstract**

29 The bifunctional protein kinase-endoribonuclease Ire1 initiates splicing of the mRNA for the
30 transcription factor Hac1 when unfolded proteins accumulate in the endoplasmic reticulum.
31 Activation of *Saccharomyces cerevisiae* Ire1 coincides with autophosphorylation of its
32 activation loop at S840, S841, T844, and S850. Mass spectrometric analysis of Ire1 expressed
33 in *Escherichia coli* identified S837 as another potential phosphorylation site *in vivo*. Mutation
34 of all five potential phosphorylation sites in the activation loop decreased, but did not
35 completely abolish, splicing of *HAC1* mRNA, induction of *KAR2* and *PDII* mRNAs, and
36 expression of a β -galactosidase reporter activated by Hac1ⁱ. Phosphorylation site mutants
37 survive low levels of ER stress better than *IRE1* deletions strains. *In vivo* clustering and
38 inactivation of Ire1 are not affected by phosphorylation site mutants. Mutation of D836 to
39 alanine in the activation loop of phosphorylation site mutants nearly completely abolished
40 *HAC1* splicing, induction of *KAR2*, *PDII*, and β -galactosidase reporters, and survival of ER
41 stress, but had no effect on clustering of Ire1. By itself, the D836A mutation does not confer a
42 phenotype. These data argue that D836 can partially substitute for activation loop
43 phosphorylation in activation of the endoribonuclease domain of Ire1.

44 **Introduction**

45 Accumulation of unfolded proteins in the endoplasmic reticulum (ER) activates the
46 bifunctional transmembrane protein kinase-endoribonuclease Ire1 (1, 2). In ER-stressed cells
47 Ire1 oligomerises (3, 4) and concentrates in clusters at the ER membrane (5, 6) independent
48 of its protein kinase activity (6, 7). In the yeast *Saccharomyces cerevisiae*, activated Ire1
49 cleaves the mRNA for the transcription factor *HAC1* to initiate removal of a 252 nt intron
50 from *HAC1* mRNA (8-11) that inhibits translation of unspliced *HAC1* (*HAC1^u*) mRNA (12).
51 Ligation of the 5' and 3' exons of *HAC1* mRNA by tRNA ligase produces spliced *HAC1*
52 mRNA (*HAC1ⁱ*) (13), which is readily translated. Hac1ⁱ induces transcription of genes

53 encoding ER-resident molecular chaperones and protein foldases, such as *BiP/KAR2* and
54 *PDII*, to alleviate the unfolded protein burden in the ER (14, 15). Many Hac1ⁱ target genes
55 contain a short promoter element, termed the unfolded protein response element (UPRE)
56 (16), to which Hac1ⁱ binds as a heterodimer with the transcription factor Gcn4 (17).

57 The N-terminal lobe of protein kinases harbours an activation segment, whose start and
58 end points are defined by the conserved amino acid sequence motifs DFG and APE in *S.*
59 *cerevisiae* Ire1. The activation segment encompasses the Mg²⁺-binding loop, a short β strand,
60 β 9 [β 10 in Ire1, (18)], the activation loop, and the P+1 loop (Fig. 1) (19). Phosphorylation in
61 the activation loop activates many protein kinases (20). Phosphorylation-dependent protein
62 kinases often display an invariant arginine (R796 in Ire1) that precedes the catalytic aspartate,
63 D797 in Ire1 (20). Crystallographic examination of active conformations of these RD kinases
64 has revealed that phosphoamino acids in the activation loop are in contact with a basic pocket
65 formed by the invariant arginine, a basic amino acid located in β 9 (β 10 in Ire1), and often a
66 third basic amino acid located in helix α C in the N-terminal lobe (19, 20). The invariant
67 arginine, R796, preceding the catalytic aspartate, D797, and a lysine in β 10, K833, have been
68 conserved throughout evolution in Ire1 (Fig. 1). Mass spectrometric mapping of tryptic
69 peptides revealed four potential phosphorylation sites in Ire1, S840, S841, T844, and S850
70 (18). Mutational analyses illustrate the importance of phosphorylation of Ire1 *in vivo*. A
71 S840A S841A double mutant displayed a large defect in induction of both *KAR2* and *PDII*
72 mRNAs (3), while *HAC1* splicing by a S840A S841A T844A triple mutant and survival of
73 ER stress by a S840A S841A T844A S850A quadruple mutant were severely decreased (18,
74 21). In addition, phosphorylation of human IRE1 α increased its RNase activity towards a
75 short, fluorescently-labelled stem loop substrate ~100-fold (22).

76 However, *HAC1* splicing in cells expressing S840A-S841A-T844A-Ire1 nevertheless
77 reached ~20% of the level of *HAC1* splicing in cells expressing WT Ire1 (21), which suggests

78 that the S840A S841A T844A mutant transduces a weak ER stress signal. In addition,
79 mutation of catalytic amino acids in the protein kinase active site, for example in D828A and
80 D797A K799A mutants, decreases, but does not abolish, processing of *HAC1* mRNA by Ire1
81 (7, 21). Finally, addition of the non-phosphorylatable ATP analogue 1-*tert*-butyl-3-
82 naphthalen-1-ylmethyl-1*H*-pyrazolo[3,4-*d*]pyrimidin-4-ylamine to cells expressing protein
83 kinase deficient mutants restored the ability to process *HAC1* mRNA (23). These
84 observations suggest that activation loop phosphorylation is dispensable for, at least partial,
85 activation of Ire1. The purpose of this study was to elucidate mechanisms that allow Ire1 to
86 transduce an ER stress signal in the absence of phosphorylation in its activation segment. Our
87 work identifies an additional potential phosphorylation site in the activation segment, S837.
88 A mutant lacking all phosphorylation sites in the activation segment, including S837, still
89 transduces a weak ER stress signal. The ability to transduce this weak ER stress signal
90 requires the presence of an aspartate, D836, in the activation loop.

91 **Materials and Methods**

92 **Plasmid constructions.** Plasmids were maintained in *Escherichia coli* XL10-Gold cells
93 (Agilent Technologies, Stockport, UK, cat. no. 200314). Standard protocols were used for
94 plasmids constructions. The single copy *URA3* plasmid pJK59 (24) for expression of Sec63-
95 GFP was obtained from W. A. Prinz (National Institute of Diabetes and Digestive and Kidney
96 Diseases, National Institutes of Health, Bethesda).

97 YCplac33-S840A-S841A-T844A-S850A-*IRE1*-HA (brief YCplac33-Q-A-*IRE1*-HA) was
98 generated by cloning the 2,002 bp *AfeI*-*MscI* fragment of pC3060-S840A-S841A-T844A-
99 S850A (18) into *AfeI*- and *MscI*-digested YCplac33-*IRE1*-HA (23). To generate YCplac33-
100 S837A-S840A-S841A-T844A-S850A-*IRE1*-HA (brief YCplac33-P-A-*IRE1*-HA) the 310 bp
101 *PstI*-*SacI* fragment of YCplac33-Q-A-*IRE1*-HA was inserted into *PstI*- and *SacI*-digested
102 pUC18 (25) and the S837A point mutation introduced by QuikChange site-directed

103 mutagenesis (Agilent Technologies) with primers H8293 and H8294 (Table 1). After
104 confirmation of the mutagenised sequence by Sanger sequencing, the 3,103 bp *PstI-SacI*
105 fragment was inserted into *PstI*- and *SacI*-digested YCplac33-Q-A-*IRE1*-HA (23). To
106 introduce the D836A mutation into wild type (WT) Ire1 and S840A-S841A-Ire1 the 1,405 bp
107 *HindIII-SacI* fragments of YCplac33-*IRE1*-HA and YCplac-S840A-S841-*IRE1*-HA (23)
108 were cloned into *HindIII*- and *SacI*-digested pUC18, followed by introduction of the D836A
109 mutation by Quik-Change site-directed mutagenesis with primers H8623 and H8624 in the
110 case of WT Ire1 and primers H8625 and H8626 in the case of S840A-S841A-Ire1. After
111 confirmation of the mutagenised sequence by Sanger sequencing, the 1,405 bp *HindIII-SacI*
112 fragments of the two pUC18 plasmids were cloned into YCplac33-*IRE1*-HA to produce
113 YCplac33-D836A-*IRE1*-HA and YCplac33-D836A-S840A-S841A-*IRE1*-HA, respectively.
114 To introduce the D836A mutation into Q-A- and P-A-Ire1, the 1,578 bp *BamHI-KpnI*
115 fragment of pGEX-1 λ T-Q-A-C'*IRE1* (Šestak *et al.*, unpublished) was cloned into *BamHI*-
116 and *KpnI*-digested pUC18 and the 69 bp *EcoRV-PstI* fragment replaced with annealed and
117 phosphorylated deoxyoligonucleotides H8627 and H8628 or annealed and phosphorylated
118 deoxyoligonucleotides H8629 and H8630. The 1,578 bp *KpnI-BamHI* fragments of the
119 resulting plasmids were cloned into *BamHI*- and *KpnI*-digested pAW42 (26). From the two
120 resulting plasmids, pGEX-1 λ T-Q-A-C'*IRE1* and pGEX-1 λ T-P-A-C'*IRE1*, the 310 bp *PstI*-
121 *SacI* fragments were cloned into *PstI*- and *SacI*-digested YCplac33-Q-A-*IRE1*-HA to
122 generate YCplac33-D836A-Q-A-*IRE1*-HA and YCplac33-D836A-P-A-*IRE1*-HA.
123 For tagging Ire1 with mCherry the 2,013 bp *AfeI-SacI* fragment of pEvA97 (5) was cloned
124 into the corresponding *AfeI*- and *SacI*-digested YCplac33-*IRE1*-HA plasmids. Then the 3,356
125 bp *HindIII-NheI* fragments of the resulting YCplac33-*IRE1*-HA plasmids were reinserted into
126 pEvA97 because mCherry fluorescence was not detectable in unstressed cells when the
127 mCherry-Ire1 fusion protein was expressed from YCplac33 in initial experiments. pGEX-

128 1λT-L745A-C'IRE1 was constructed by amplifying a 1,277 bp PCR product with primers
129 8619G and H4075A04 from YCplac33-L745A-*IRE1* (23), and cloning the *Bam*HI- and *Pml*I-
130 digested PCR product into *Bam*HI- and *Pml*I-digested pAW42.

131 For galactose-inducible expression of HA- and protein A-tagged Dcr2 and Ptc2, the 2,777
132 bp and 2,435 *Bss*HII fragments of BG1805-*DCR2* and BG1805-*PTC2* (27) were ligated to the
133 6,692 bp *Bss*HII fragment of pRSII422 (28) or the 6,676 bp *Bss*HII fragment of pRS425 (29).
134 H338A-Dcr2 (30) and E37A-D38A-Ptc2 (31) were generated by QuikChange site-directed
135 mutagenesis with primer pairs DCR2-H338A-F and DCR2-H338A-R and PTC2-E37A-
136 D38A-F and PTC2-E37A-D38A-R (Table 1) on BG1805-*DCR2* and BG1805-*PTC2*,
137 respectively. After confirmation of the mutagenised sequences by Sanger sequencing, the
138 1,070 bp *Cla*I-*Eag*I fragment of BG1805-H338A-*DCR2* was cloned into *Cla*I- and *Eag*I-
139 digested pRSII422-*DCR2* and the 1,153 bp *Sac*I-*Xho*I-fragment of BG1805-E37A-D38A-
140 *PTC2* was cloned into *Sac*I- and *Xho*I-digested pRSII422-*PTC2* and from there the 2,777 bp
141 *Bss*HII fragments of pRSII422-*DCR2* and pRSII422-H338A-*DCR2* and the 2,435 bp *Bss*HII-
142 fragments of pRSII422-*PTC2* and pRSII422-E37A-D38A-*PTC2* were cloned into *Bss*HII-
143 digested pRS425.

144 **Yeast methods.** Yeast strains (Table 2) were transformed by the LiOAc method (32). *Ire1*
145 was deleted in W303-1A (33) as described previously (34). *DCR2* and *PTC2* were deleted by
146 PCR-based gene disruption (35) with primer pairs H9327 and H9328 and H9329 and H9330
147 (Table 1) and pFA6a-*kanMX2* (35) or pFA6a-*hphNT1* (36) as template. The *GAL1* promoter
148 and a N-terminal T7 epitope tag were introduced by transforming PWY 260 with PCR
149 constructs amplified with primer pairs H9328 and H9331 and H9330 and H9332 from
150 plasmid pFA6a-*kanMX6-P_{GALI}-T7*. pFA6a-*kanMX6-P_{GALI}-T7* was constructed by inserting
151 annealed and kinased oligonucleotides U5803H01 and U5803H02 into *Pac*I- and *Bam*HI-
152 digested pFA6a-*kanMX6-P_{GALI}* (37). The T7 sequence in pFA6a-*kanMX6-P_{GALI}-T7* was

153 confirmed by Sanger sequencing. In frame fusion of the T7 epitope tag to the *DCR2* and
154 *PTC2* open reading frames was confirmed by Sanger sequencing.

155 To induce ER stress, cells were grown to mid-exponential growth phase on synthetic
156 dextrose (SD) medium lacking uracil or leucine (38). 1,4-DL-Dithiothreitol (DTT) was added
157 to a final concentration of 2 mM from a 1 M stock solution made in water. To wash out DTT,
158 cells treated with 2 mM DTT for 2 h were washed once with SD medium lacking uracil and
159 then resuspended in the same culture volume of fresh SD medium lacking uracil. For
160 fluorescence microscopy the concentrations of adenine and L-tryptophan were raised to 100
161 mg/l. Survival of ER stress was scored by spotting 2 μ l of serial ten-fold dilutions of fresh
162 overnight cultures onto freshly prepared synthetic media agar plates lacking uracil and
163 containing 2% (w/v) glucose as carbon source. Expression of *DCR2* and *PTC2* from the
164 *GALI* promoter was induced by growing the cells from single colonies in a small volume of
165 synthetic medium with 1% (w/v) raffinose and 2% (w/v) galactose as carbon source lacking
166 uracil, both uracil and adenine, or both uracil and leucine. Cells were then spotted onto
167 synthetic media plates containing 1% (w/v) raffinose and 2% (w/v) galactose for ER stress
168 survival assays. All overnight cultures were adjusted to optical densities at 600 nm of 3.0
169 before preparing serial ten-fold dilutions. To semiquantitatively evaluate growth assays,
170 threshold dilutions, D_T , were defined as the maximum dilutions at which growth could be
171 observed and were determined with an accuracy limit of ~ 0.5 . The difference between the
172 two negative decadic logarithms of the threshold dilutions for tunicamycin exposed cells and
173 untreated cells, $\Delta \log D_T$, is defined as $\Delta \log D_T = -\log D_{T,Tm} - (-\log D_{T,u})$, where $D_{T,Tm}$ is the
174 threshold dilution of tunicamycin-exposed cells and $D_{T,u}$ the threshold dilution of untreated
175 cells. Only differences in $\Delta \log D_T \geq 0.5$ were considered to be significant.

176 **Northern analysis.** Northern blotting was performed as described previously (34), except
177 that cells were lysed by bead-beating with 0.5 mm diameter glass beads (Stratech Scientific,

178 Newmarket, UK, cat. no. 11079105z) in a Precellys 24 instrument (Bertin Technologies,
 179 Montigny-le-Bretonneux, France) at 4°C with two cycles of 30 s at 6,500 rpm separated by a
 180 30 s break. The probes for *HAC1* (34), *KAR2* (39), *PDII* (39), and the loading control pC4/2
 181 (40) were described previously. All mRNAs were quantified by phosphorimaging on a
 182 Typhoon 9400 system (GE Healthcare, Little Chalfont, UK). Volumetric measurements were
 183 normalised to the loading control pC4/2. The percentage of *HAC1*^{*i*} (% *HAC1*^{*i*}) is defined as

$$\% \text{HAC1}^i = \frac{\text{HAC1}^i}{\text{HAC1}^u + \text{HAC1}^i + 1^{\text{st}} \text{ exon \& intron} + 1^{\text{st}} \text{ exon}}$$

184 The percentage of *HAC1* cleavage (% cleavage) is defined as

$$\% \text{Cleavage} = \frac{\text{HAC1}^i + 0.5 \cdot (1^{\text{st}} \text{ exon \& intron} + 1^{\text{st}} \text{ exon})}{\text{HAC1}^u + \text{HAC1}^i + 1^{\text{st}} \text{ exon \& intron} + 1^{\text{st}} \text{ exon}}$$

185 **β-Galactosidase reporter assays** were performed as described before (39). Cells were grown
 186 to mid-exponential phase, a zero hour sample collected, and the remainder of the culture
 187 exposed to 2 mM DTT and further samples collected after 1 h and 2 h. After washing cells
 188 with ice-cold water, protein extracts were produced in 1 x reporter lysis buffer (Promega,
 189 Southampton, UK, cat. no. E3971) by bead-beating with 0.5 mm diameter glass beads in a
 190 Precellys 24 instrument at 4°C with 3 cycles of 10 s at 6,500 rpm. Between each cycle
 191 samples were cooled for 5 min on ice. The lysates were centrifuged at 12,000 g and 4°C for
 192 10 min and supernatants were transferred into fresh microcentrifuge tubes to obtain protein
 193 extracts. β-Galactosidase activity was standardised to total protein determined with the DC
 194 protein assay from Bio-Rad Laboratories (Hemel Hempstead, UK, cat. no. 500-0116).

195 **Protein extraction and Western blotting.** Mid-exponential growth phase cells were washed
 196 once with 5 ml of ice-cold water, once with 1 ml ice-cold water and then resuspended in 200
 197 μl 8 M urea, 2.5 % (w/v) SDS, 50 mM Tris·HCl, pH 7.5 (at 4°C), 6 mM EDTA, 5 mM
 198 β-mercaptoethanol, 2 mM phenylmethanesulphonyl fluoride (PMSF), and 6 mM 4-(2-
 199 aminoethyl)-benzenesulphonyl fluoride (AEBSF). The cells were lysed by bead-beating as

200 described for the β -galactosidase reporter assays. Protein concentrations were quantified with
201 bicinchoninic acid (41) after alkylation of β -mercaptoethanol with 0.1 M iodoacetamide in
202 0.1 M Tris·HCl, pH 8.0 at 37°C for 15 min.

203 Proteins (50 μ g) were separated on 8% SDS-PAGE gels (42) and transferred to
204 polyvinylidene difluoride (PVDF) membranes (Amersham HyBondTM- P, pore size 0.45 μ m,
205 GE Healthcare, Little Chalfont, UK, cat. no. RPN303F) by semi-dry electrotransfer in 0.1 M
206 Tris, 0.192 M glycine and 5% (v/v) methanol at 2 mA/cm² for 75 min. Membranes were
207 stained with 0.5% (w/v) Ponceau S in 1% (v/v) acetic acid for 5 min at RT, destained 3 x 2
208 min with water, dried on air, and photographed. Membranes were then blocked overnight in
209 5% (w/v) skimmed milk powder in TBST [20 mM Tris·HCl, pH 7.6 (at RT), 137 mM NaCl,
210 and 0.1% (v/v) Tween-20] at 4°C and then incubated with a 1:1,000 dilution of rabbit anti-
211 HA antibody (Sigma-Aldrich, Poole, UK, cat. no. H6908, batch no. 015M4868V) in TBST +
212 5% (w/v) skimmed milk powder for 2 h at RT. Blots were washed four times with TBST and
213 then probed with a 1:2,000 dilution of anti-rabbit IgG (H+L)-peroxidase conjugate (Cell
214 Signaling Technology Inc., Danvers, MA, USA, cat. no. 7074S, batch no. 24) in TBST + 5%
215 (w/v) skim milk powder for 1 h at RT. Blots were then washed four times with TBST and
216 developed by enhanced chemiluminescence as described before (43). To probe blots for the
217 actin loading control, blots were stripped after enhanced chemiluminescence detection by
218 washing them twice for 5 min with 100 mM Tris·HCl, pH 8.5 (at RT) and 0.1% (v/v) Tween-
219 20, twice for 15 min with 100 mM Tris·HCl, pH 8.5 (at RT), 200 mM β -mercaptoethanol,
220 and 0.1% (v/v) Tween-20, twice for 5 min with TBST, twice for 15 min with 100 mM
221 glycine, pH 2.5 (at RT) and 0.1% (w/v) Tween-20 at 37°C, and twice for 15 min with TBST.
222 Blots were then blocked overnight at 4°C with 5% (w/v) skimmed milk powder in TBST and
223 then incubated for 1 h at RT with a 1:1·10⁵ dilution of a mouse anti- β -actin antibody (Abcam,
224 Cambridge, UK, cat. no. ab170825, batch no. GR184354-8) in TBST + 5% (w/v) skimmed

225 milk powder. Blots were washed four times with TBST, incubated for 1 h at RT with a
226 $1:2 \cdot 10^5$ dilution of a goat anti-mouse IgG (H+L) peroxidase conjugate (Thermo Fisher
227 Scientific, Loughborough, UK, cat. no. 31432, batch no. OE17149612) in TBST + 5% (w/v)
228 skimmed milk powder, washed again four times with TBST, and developed by enhanced
229 chemiluminescence. Films were scanned on a MFC-5320DW all-in-one printer (Brother
230 Industries, Manchester, UK) and saved as tif files. Bands were quantified using CLIQS 1.1
231 (Totallab, Newcastle upon Tyne, UK).

232 **Protein expression and purification.** The cytosolic domains of WT and L745A-Ire1 starting
233 at amino acid 556 were expressed as *N*-terminal GST fusion proteins from plasmid pGEX-
234 1λ T (Genbank accession no. U13849) by autoinduction (44) in *E. coli* BL21-
235 CodonPlus(DE3)-RIL cells (Agilent Technologies, cat. no. 230240). These constructs
236 encompass the complete linker, serine/threonine protein kinase, and RNase domains of Ire1.
237 A ZYM-5052 culture containing 50 μ g/ml ampicillin and 25 μ g/ml chloramphenicol was
238 inoculated with 1/1000 volume of a fresh overnight culture grown in MDG medium, grown at
239 37°C for 5 h and then a further 28 h at 20°C (44). The cells were harvested by centrifugation
240 at 4,750 g and 4°C for 15 min and washed twice with ice-cold 0.2 M Tris·HCl, pH 8.0 (at
241 4°C), and finally resuspended in 0.2 M Tris·HCl, pH 8.0 (at 4°C), 0.5 M sucrose, one tablet
242 of Roche complete protease inhibitors lacking EDTA (Roche Applied Sciences, Burgess Hill,
243 UK, cat. no. 11873580001), 2 mM PMSF, 6 mM AEBSF, and 1 μ g/ml pepstatin. The cells
244 were lysed by addition of 10 μ g/OD_{600 nm} chicken lysozyme (Sigma-Aldrich, cat. no. 62971),
245 addition of EDTA to a final concentration of 1 mM, dilution of the cell suspension with one
246 volume of H₂O, and incubation of the cell suspension on a roller mixer for 10 min at room
247 temperature. After addition of 1/10 Vol. of 10% (v/v) Triton X-100 the cell suspension was
248 sonicated in a Soniprep 150 sonicator (MSE Ltd., London, UK) with a 19 mm diameter probe
249 in an ice/NaCl bath for twelve cycles of 1 min sonication with an amplitude of 0.22 microns

250 followed by a cooling period, in which the cell suspension was allowed to cool to 4°C. The
251 lysate was then cleared by centrifugation at 40,000 g and 4°C for 15 min. The GST-Ire1
252 fusion protein was purified by affinity chromatography on GSTrap 4B sepharose columns
253 (GE Healthcare, cat. no. 28-4017-45) and eluted from the column with 20 mM Tris·HCl, pH
254 7.5 (at 4°C), 100 mM NaCl, 5% (v/v) glycerol, 0.1% (w/v) CHAPS, 1 mM EDTA, 2 mM
255 PMSF, and 10 mM glutathione. The eluted protein was concentrated in Amicon Ultra-15
256 centrifugal filters (MWCO 50 kDa, Merck Millipore, cat. no. UFC905008) and desalted on a
257 HiTrap desalting column (GE Healthcare, cat no. 17-1408-01).

258 **Mass spectrometric (MS) identification of Ire1 autophosphorylation sites.** 5 µg of the
259 cytosolic domains of WT and L745A-Ire1 expressed as GST fusion proteins in *E. coli* and
260 purified by affinity chromatography on GSTrap 4B columns as described above were run on
261 an 8% SDS-PAGE gel and stained with Coomassie Brilliant Blue R250. Coomassie-stained
262 protein bands were excised from the gel, transferred to a microtitre plate and destained, buffer
263 exchanged, reduced with DTT, alkylated with iodoacetamide, and digested with trypsin using
264 an automated digestion robot (DiGiLab, Genomic Solutions, Ann Arbor, MI, USA) as
265 described before (45).

266 MS/MS analysis of the cytosolic domains of WT and mutant Ire1 expressed in *E. coli* was
267 carried out on an LTQ XL orbitrap mass spectrometer (Thermo Scientific) coupled to an
268 Ultimate 3000 nano HPLC system. The RP-LC system consisted of a desalting column (300
269 µm x 5 mm, PepMap C18 3 µm, 100 Å) and an analytical column (75 µm x 250 mm,
270 PepMap C18 3 µm, 100 Å) with split solvent delivery (split ratio 1:300). A Thermo
271 nanospray II source was fitted with a 30 µm silica emitter tip (PicoTip, New Objective, US)
272 and maintained at 1100 V ion spray voltage. Peptide samples (3 µl) were loaded onto the trap
273 column in 0.1% (w/v) trifluoroacetic acid at 20 µl/min for 3 min and eluted at 300 nl/min
274 using a gradient from 0.05% (v/v) formic acid in water (A) to 0.05% formic acid in 80% (v/v)

275 acetonitrile (B). The gradient profile was as follows: 4% buffer B for 3 min, 4% B to 40% B
276 in 40 min, 40% B to 65% B in 6 min, 65% B to 95% B in 1 min, and 95% B for 6 min. Using
277 Excalibur 2.0.1, intact peptides were detected between m/z 400 and m/z 1,600 in the orbitrap
278 at a resolution of 60,000. Internal calibration was performed using the ion signal of
279 $(\text{Si}(\text{CH}_3)_3\text{O})_6\text{H}^+$ at m/z 445.120025 as a lock mass (46). Maximum ion accumulation time
280 allowed on the LTQ orbitrap was 1 s for all scan modes. Automatic gain control was used to
281 prevent over-filling of the ion trap. Collision induced dissociation (CID) spectra of the top 5
282 peptide ions (minimum intensity 10,000 counts, rejection of singly charged precursors) were
283 acquired at a normalised collision energy of 35. Dynamic exclusion was set with a repeat
284 count of 1, a repeat time of 30 s and, an exclusion time of 3 min and an exclusion list size of
285 50. The chromatography feature was enabled with a correlation area ratio of 1.0. Activation
286 Q was set to 0.25 with 30 ms activation time.

287 XITandem tornado version 2009.04.01.1 (47) was used to search the ENSEMBL yeast
288 proteome database (version SGD1.01.55) and the common repository of adventitious proteins
289 (cRAP, <http://www.thegpm.org/crap/index.html>) for the identification of proteins and the
290 reversed version of both databases. Precursor mass accuracy was set to 20 ppm and fragment
291 mass error to 0.6 Da. Carbamidomethylation of cysteine was set as a fixed modification and
292 phosphorylation of serine, threonine and tyrosine as a variable modification. At the
293 refinement step, oxidation of methionine and tryptophan, double oxidation of methionine and
294 tryptophan, deamidation of asparagine and glutamine, methylation of aspartate, glutamate,
295 histidine, lysine, arginine and asparagine, carbamidomethylation of lysine, histidine, aspartate
296 and glutamate and dehydration of serine and threonine were included in the search
297 parameters. At a cutoff \log_e value of 1.0, searching the decoy databases indicated a false
298 discovery rate between 1.18% and 1.39% for protein identification. Detailed results and all
299 spectra can be accessed via the following links: WT - <http://human.thegpm.org/thegpm->

300 [cgi/plist.pl?path=/tandem/archive/GPM28700000061.xml](http://human.thegpm.org/thegpm-cgi/plist.pl?path=/tandem/archive/GPM28700000061.xml) and L745A -

301 <http://human.thegpm.org/thegpm-cgi/plist.pl?path=/tandem/archive/GPM28700000059.xml>.

302 The mass spectrometry proteomics data have been deposited to the ProteomeXchange
303 Consortium via the PRIDE (48) partner repository with the dataset identifier PXD004924.

304 **Confocal fluorescence microscopy.** Cells grown to mid-exponential growth phase in SD
305 medium lacking leucine and uracil and supplemented with 100 mg/l adenine and 100 mg/l L-
306 tryptophan were concentrated ~60 fold in SD medium lacking leucine and uracil and
307 supplemented with 100 mg/l adenine and 100 mg/l L-tryptophan before addition of 2 mM
308 DTT. 5 µl of untreated cell suspensions or cell suspensions exposed to 2 mM DTT were
309 examined on a Zeiss LSM 880 with Airyscan confocal inverted microscope (Carl Zeiss Ltd.
310 Cambridge, UK) using a Plan-Apochromat 63x/1.4 Oil DIC M27 objective and a MDS
311 488/594 beam splitter. GFP fluorescence was excited with a 488 nm laser at a power setting
312 of 5 – 8% and its fluorescence emission was collected between 498 to 564 nm with a
313 photomultiplier tube. mCherry fluorescence was excited with a 594 nm laser at a power
314 setting of 28 – 40% and its fluorescence emission was collected at 694 – 754 nm with a
315 gallium arsenide phosphide detector. Gain settings between 650 and 900 were used to collect
316 images.

317 **Statistical analyses.** Experimental data are presented as the mean and its standard error. For
318 composite parameters, errors were propagated using the law of error propagation for random,
319 independent errors (49). All data were analysed for normality using the D'Agostino-Pearson
320 omnibus normality test (50), equality of variances (homoscedasticity) using the Brown-
321 Forsythe test (51) or Bartlett's test (52), and for additivity of means, treatment effects, and
322 errors using Tukey's test (53, 54) before ANOVA. Heteroscedastic or nonadditive data were
323 ln-transformed before ANOVA (53) or analysed by Welch's test (55) followed by the
324 Games-Howell post-hoc test (56). Normality was examined on the pooled data for the *ire1Δ*

325 deletion strain transformed with YCplac33 or, alternatively, on all pooled data points before
326 induction of ER stress. In all analyses $P \leq 0.05$ was considered to be statistically significant.
327 Brown-Forsythe tests for equality of variances, Tukey's test for additivity, Welch's tests, and
328 Games-Howell post hoc tests were performed in Microsoft Excel 2010 (Microsoft
329 Corporation, Redmond, WA, USA) using the Real Statistics plug-in for Microsoft Excel
330 (<http://www.real-statistics.com/>). All other statistical calculations were performed in
331 GraphPad Prism 6.07 (GraphPad Software, La Jolla, CA, USA).

332 **Results**

333 *S837 is a potential autophosphorylation site.* To identify autophosphorylation sites in the
334 activation segment of Ire1, we expressed the cytosolic portion of Ire1 starting at Q556 as an
335 N-terminal glutathione S transferase fusion protein in *E. coli*, purified it by affinity
336 chromatography on glutathione sepharose beads and analysed tryptic digests by tandem mass
337 spectrometry. Four peptides that cover the activation segment from L835 to R856 carrying
338 one phosphoryl group at S841 (spectrum 1155, data not shown), two phosphoryl groups at
339 S841 and T844 (spectrum 1475, data not shown), three phosphoryl groups at S840, S841, and
340 S850 (spectrum 1976, Fig. 2A), and three phosphoryl groups at S840, T844, and S850
341 (spectrum 2031, Fig. 2B) were identified. In addition, a shorter peptide starting at T844 and
342 carrying one phosphoryl group at S850 was identified (spectra 760 and 816, data not shown).
343 These autophosphorylation sites in the activation segment of WT Ire1 correspond to
344 previously reported autophosphorylation sites in the activation segment (18).

345 We also characterised autophosphorylation of an L745A mutant of Ire1, which possesses
346 an enlarged ATP binding pocket to accommodate chemically-modified, bulkier adenine
347 moieties (57, 58). *In vivo*, L745A-Ire1 supports induction of an UPRE-*lacZ* reporter to ~60%
348 of WT levels (23), which suggests that this mutant possesses significant protein kinase and
349 RNase activities. MS/MS analyses of tryptic peptides derived from the L745A mutant

350 identified several peptides that cover the activation segment from L835 to R856. One carried
351 three phosphoryl groups at S840, S841, and T844 (spectrum 1583, data not shown), another
352 carried four phosphoryl groups at S840, S841, T844, and S850 (spectrum 2251, data not
353 shown), and a third one also carried four phosphoryl groups (spectrum 2263, data not shown).
354 Of these, three could be unambiguously assigned to S840, S841, and T844, while the fourth
355 phosphoryl group is located on S850 or T852. No peptide allowed unambiguous assignment
356 of a phosphoryl group to T852. A peptide that covers the activation segment from K834 to
357 R856 carried two phosphoryl groups at S837 and T844, one phosphoryl group at S840 or
358 S841 and another phosphoryl group at S850, T852, or S853 (spectrum 1462, Fig. 2C).
359 Evidence for phosphorylation at S837 is provided by the m/z ratio of the ^{+1}b ion of m/z
360 709.033 Da, which exceeds the m/z ratio for the unphosphorylated peptide by 79.7 Da. This
361 difference matches, within the measurement error of 0.6 Da, the mass difference between a
362 phosphorylated and unphosphorylated peptide. In addition to peptides carrying multiple
363 phosphoryl groups two monophosphorylated peptides, one covering the activation segment
364 from L835 to R843 and being phosphorylated at S841 (spectrum 152, data not shown) and
365 one covering the activation segment from T844 to R856 and being phosphorylated at S850
366 (spectra 488 and 540, data not shown) were detected. These data show that
367 autophosphorylation of WT and L745A Ire1 in the activation segment strongly overlap and
368 raise the possibility that S837 is an additional autophosphorylation site in the activation
369 segment of Ire1.

370 *Mutation of all phosphorylation sites in the activation segment decreases, but does not*
371 *eliminate, HAC1 splicing, induction of ER chaperone genes, and survival of ER stress. To*
372 *evaluate the contribution of S837 to activation of Ire1 we characterised the ER stress*
373 *response of three Ire1 mutants, S840A S841A, S840A S841A T844A S850A (brief: Q-A),*
374 *and S837A S840A S841A T844A S850A (brief: P-A). A time course experiment revealed*

375 that *HAC1* splicing reaches steady-state levels as early as 15 min after induction of ER stress
376 with 2 mM DTT in cells in the mid-exponential growth phase (Fig. 3A-C). An increase in
377 *HAC1* splicing 15 min after induction of ER stress was detectable in all three mutants, but
378 was quantitatively lower than in cells expressing WT Ire1. Differences between the three
379 phosphorylation site mutants were not statistically significant (Fig. 3B, C). 2 h after induction
380 of ER stress the difference between cells lacking Ire1 and cells expressing either S840A-
381 S841A-Ire1 or Q-A-Ire1 were statistically significant (Fig. 3B, C), whereas the difference
382 between cells lacking Ire1 and cells expressing P-A-Ire1 did not become statistically
383 significant (Fig. 3B, C). These two comparisons, cells expressing P-A-Ire1 to cells expressing
384 S840A-S841A- or Q-A-Ire1 and cells expressing P-A-Ire1 to cells lacking Ire1, suggest that
385 S837 may make a minor contribution to activation of Ire1.

386 The differences in *HAC1* splicing were reflected by the induction of *KAR2* and *PDII*
387 mRNAs. Induction of both mRNAs kinetically trailed *HAC1* splicing and reached a
388 maximum only after ~1 h of ER stress (Fig. 3A, D-E). All three phosphorylation site mutants
389 induced both *KAR2* and *PDII* mRNAs to similar levels, which remained, especially in the
390 case of *KAR2* mRNA, below the level of induction reached in cells expressing WT Ire1. 2 h
391 after induction of ER stress with 2 mM DTT *KAR2* mRNA, but not *PDII* mRNA levels, were
392 significantly increased in all autophosphorylation site mutants when compared to cells
393 lacking Ire1, suggesting that even P-A-Ire1 can partially activate expression of *KAR2* in ER-
394 stressed cells.

395 Next, we compared expression of an UPRE-*lacZ* reporter between cells expressing the
396 different autophosphorylation site mutants, because accumulation of the comparatively stable
397 protein β -galactosidase (59) may reveal subtle differences in transduction of the ER stress
398 signal. All three autophosphorylation site mutants induced expression of the reporter, but to a
399 lower degree than cells expressing WT Ire1 (Fig. 4A, B). This observation suggests that Ire1

400 can transduce an ER stress signal in the absence of autophosphorylation in its activation loop.
401 Induction of the *lacZ* reporter was stronger in cells expressing S840A-S841A-Ire1 than in
402 cells expressing either Q-A- or P-A-Ire1 (Fig. 4A), which supports the conclusion that
403 phosphorylation of S837, T844, or S850 contributes to activation of Ire1 at least when
404 phosphorylation at S840 and S841 is no longer possible.

405 To explore the possibility that decreased *HAC1* splicing and *KAR2* and *PDII* mRNA
406 induction by activation loop mutants is caused by a defect in clustering of Ire1 *in vivo* (5), we
407 monitored foci formation by WT and mutant Ire1 fused to the fluorescent protein mCherry
408 before and after induction of ER stress with 2 mM DTT for 15 min or 60 min. Before
409 induction of ER stress Ire1-mCherry displayed a distribution characteristic for an ER protein
410 with areas of fluorescence around the nucleus and the cell surface, which are indicative of the
411 perinuclear and cortical ER (Fig. 5). This distribution also overlapped with the distribution of
412 a fluorescent marker for the ER, a fusion of GFP to the C-terminus of the Sec63 subunit of
413 the protein translocation channel of the ER membrane (24). In addition to this ER
414 localisation, cells carrying WT and mutant *IRE1* alleles also showed a distinct intracellular
415 mCherry fluorescence that filled most of the cell body (Fig. 5). This mCherry fluorescence
416 colocalises with the fluorescence of the vacuolar stain 7-amino-4-chloromethylcoumarin
417 (data not shown). As early as 15 min after induction of ER stress with 2 mM DTT, a
418 characteristic punctuate fluorescence developed for the mCherry, but not the GFP
419 fluorescence in cells expressing WT Ire1-mCherry. This punctuate fluorescence is indicative
420 of clustering of Ire1 *in vivo* in the ER membrane (5). 1 h after DTT treatment most of the
421 mCherry fluorescence localises to clusters (Fig. 5). There were no noticeable differences in
422 the development of punctuate mCherry fluorescence in cells expressing activation loop
423 mutants of Ire1 fused to mCherry (Fig. 5). These experiments suggest that activation loop
424 mutants do not display a defect in clustering *in vivo*.

425 To evaluate whether the weak ER stress response of the phosphorylation site mutants
426 suffices to survive ER stress, we characterised the survival of these mutants under conditions
427 of low levels of ER stress. Consistent with the gene expression data, all phosphorylation site
428 mutants displayed a small degree of protection against ER stress, as evidenced by their
429 improved growth on plates containing 0.4 $\mu\text{g/ml}$ tunicamycin when compared to cells lacking
430 Ire1 (Fig. 6). At higher concentrations of tunicamycin this growth advantage of the
431 phosphorylation site mutants over the *IRE1* deletion strain was diminished. Activation loop
432 mutants express to levels comparable to WT Ire1 in both the S288C and W303 genetic
433 backgrounds (Fig. 7 and data not shown), which suggests that the partial defect in responding
434 to ER stress displayed by activation loop mutants cannot be explained by decreased
435 intracellular abundance of mutant Ire1 proteins. In summary, these data show that all three
436 autophosphorylation site mutants can activate a weak, but physiologically significant, ER
437 stress response.

438 *D836 is required for the ER stress response mediated by phosphorylation site mutants.* The
439 activation loop of Ire1 features an aspartate that has been functionally conserved throughout
440 evolution in fungal and plant Ire1 (Fig. 1). Phosphorylation-independent RD kinases can
441 employ a negatively charged glutamate located in the activation loop to stabilise the basic
442 pocket formed by the invariant arginine and the basic amino acid located in strand $\beta 9$ (20).
443 For example, in phosphorylase kinase glutamate 182 neutralises the invariant arginine that
444 precedes the catalytic aspartate (60). Mutation of this glutamate to serine decreases catalytic
445 efficiency ~ 20 fold (61). In partially active human CDK2-cyclin A complexes the basic
446 pocket is stabilised by interaction with glutamate 162 (62). For these reasons, we introduced a
447 D836A mutation into WT Ire1 and the three phosphorylation site mutants and compared the
448 ER stress response of these mutants to the ER stress response of WT Ire1, S840A-S841A-
449 Ire1, Q-A-Ire1, and P-A-Ire1.

450 Splicing of *HAC1* mRNA and induction of both *KAR2* and *PDII* mRNA were monitored
451 in time course experiments similar to the experiments described above. Introduction of the
452 D836A mutation into WT Ire1 had no effect on *HAC1* splicing or induction of *KAR2* and
453 *PDII* mRNAs (Fig. 8). By contrast, introduction of the D836A mutation into S840A-S841A-
454 Ire1, Q-A-Ire1, or P-A-Ire1 resulted in a virtually complete loss of *HAC1*ⁱ mRNA and
455 abrogated induction of *KAR2* mRNA (Fig. 8). *PDII* mRNA no longer increased to levels
456 significantly above levels seen in cells deleted for *IRE1*. Despite of the absence of *HAC1*ⁱ
457 mRNA, faint bands representing cleavage intermediates, such as the 1st exon of *HAC1*^u
458 mRNA plus the intron and the 1st exon of *HAC1*^u mRNA could still be observed in cells
459 expressing D836A-S840A-S841A-, D836A-Q-A-, or D836A-P-A-Ire1 (Fig. 8A).

460 Introduction of the D836A mutation nearly completely eliminated expression of
461 β -galactosidase from UPRE-*lacZ* reporters when introduced into S840A-S841A- and Q-A-
462 Ire1 (Fig. 9). Introduction of the D836A mutation into P-A-Ire1 further decreased expression
463 of β -galactosidase 2 h after induction of ER stress with 2 mM DTT (from 11.2 ± 1.6 U/g to
464 5.6 ± 1.4 U/g) to levels very close to and statistically undistinguishable from levels seen in
465 *IRE1* deletion strains exposed to ER stress for 2 h (2.7 ± 0.4 U/g), but this decrease did not
466 reach statistical significance. Differences in expression levels of the β -galactosidase reporter
467 in *IRE1* deletion cells, cells expressing D836A-S840A-S841A-, D836A-Q-A-, or D836A-P-
468 A-Ire1 were not statistically significant (Fig. 7). The D836A mutation, however, did not
469 affect expression of β -galactosidase when introduced into WT Ire1 (Fig. 9). The D836A
470 mutation did also not affect clustering of Ire1 *in vivo*, either in the context of otherwise WT
471 Ire1 or the activation loop mutants (Fig. 10), or steady-state expression levels of Ire1 (Fig. 7).
472 Introduction of the D836A mutations into the phosphorylation site mutants resulted in growth
473 phenotypes very similar to the growth phenotypes of *IRE1* deletion cells (Fig. 11), but, as in
474 the case of the gene expression data the D836A mutation by itself did not decrease survival of

475 ER stress induced with tunicamycin or DTT (Fig. 11). Taken together, these data support the
476 conclusion that D836 is required for the residual ER stress response only when activation
477 loop phosphorylation is impaired.

478 *Activation loop mutants do not affect inactivation of Ire1.* To investigate whether mutations
479 in the activation loop affect the inactivation of Ire1, we characterised the decay of *HAC1*
480 splicing, *KAR2* and *PDII* mRNA after washout of DTT from cells exposed to 2 mM DTT for
481 2 h. The percentage of *HAC1*ⁱ mRNA, the percentage of *HAC1* mRNA cleavage, *KAR2* and
482 *PDII* mRNA levels decayed with first order kinetics (Fig. 12). The lower maximal responses
483 of the S840A S841A, Q-A, and P-A mutants to 2 mM DTT (Figs. 3, 8, and 12) allow these
484 mutants to return to basal levels of *HAC1* splicing, *KAR2* and *PDII* mRNA levels earlier than
485 cells expressing WT and D836A-Ire1 (Fig. 12). We did not find any statistically significant
486 differences in the decay rates for any of the Ire1 mutants in an ordinary one way ANOVA
487 with Tukey's correction for multiple comparisons. Likewise, no obvious differences between
488 WT Ire1 and any Ire1 mutants in the dissolution of Ire1 clusters at the ER membrane were
489 observed (Fig. 5 and Fig. 10). These data suggest that inactivation of Ire1 is independent of
490 D836 and phosphorylation sites in the activation loop.

491 *Negative regulation of Ire1 by the phosphatase Ptc2 requires phosphorylation sites in the*
492 *activation loop of Ire1.* The identical inactivation kinetics for WT Ire1 and activation loop
493 mutants prompted us to characterise whether two negative regulators of Ire1, the
494 phosphatases Dcr2 (30) and Ptc2 (31), negatively regulate Ire1 through its activation loop.
495 Overexpression of Ptc2 from the *GALI* promoter on a 2 μ plasmid inhibited growth (31).
496 Overexpression of WT Ptc2, but not catalytically inactive E37A-D38A- or D234A-Ptc2, also
497 inhibited growth of cells exposed to a low concentration tunicamycin (31). Consistent with
498 this earlier report, we find that overexpression of Ptc2 from the *GALI* promoter on the 2 μ
499 plasmid pRSII422 inhibited growth of unstressed cells (Fig. 13A). Overexpression of

500 catalytically inactive E37A-D38A-Ptc2 also inhibited growth of unstressed cells, but to a
501 lesser extent than overexpression of WT Ptc2 (Fig. 13A). Deletion of *IRE1* slightly impaired
502 growth of unstressed cells on raffinose and galactose, but also masked the negative effects of
503 expression of WT or E37A-D38A-Ptc2 on growth of unstressed cells (Fig. 13A). Likewise,
504 expression of D836A-P-A-Ire1 masked the negative effects of expression of WT or E37A-
505 D38A-Ptc2 on growth of unstressed cells, suggesting that WT and E37A-D38A-Ptc2 act
506 through Ire1 to inhibit growth of unstressed cells.

507 These genetic interactions between *IRE1* and *PTC2* in unstressed cells complicate the
508 interpretation of effects of overexpression of Ptc2 in ER-stressed cells expressing different
509 *IRE1* alleles. Therefore, we semiquantitatively scored the effects of overexpression of Ptc2 on
510 survival of ER stress by calculating the differences between the maximum dilutions at which
511 growth of more than two cells can be observed for ER-stressed and unstressed cells. This
512 scoring system revealed that expression of WT Ptc2, but not E37A-D38A-Ptc2, in cells
513 expressing WT or D836A-Ire1 impaired growth in the presence of ER stress induced with 0.8
514 $\mu\text{g/ml}$ tunicamycin (Fig. 13A). This observation is consistent with the earlier finding that
515 overexpression of WT, but not catalytically inactive Ptc2, inhibited growth of ER-stressed
516 cells (31). The negative effects of overexpression of WT Ptc2 on growth of ER-stressed cells
517 were abrogated in *ire1* Δ cells or cells expressing P-A- or D836A-P-A-Ire1 (Fig. 13A). These
518 data show that deletion of *IRE1* or expression of a mutant in which all potential
519 phosphorylation sites in the activation loop have been mutated to alanine mask the effects of
520 overexpression of WT Ptc2 on growth of ER-stressed cells.

521 Overexpression of Dcr2 by placing the *GALI* promoter in front of the chromosomal
522 *DCR2* gene was reported to inhibit growth when ER stress was induced with tunicamycin
523 (30). In contrast to this finding, we did not observe any inhibition of growth by
524 overexpression of Dcr2 using a similar expression system (Fig. 13B). We then explored

525 whether further elevation of Dcr2 levels by expressing Dcr2 from the *GALI* promoter on the
526 2 μ plasmid pRSII422 affects growth of ER-stressed cells, because overexpression of Ptc2
527 from the *GALI* promoter on a 2 μ plasmid inhibited growth of ER-stressed cells (Fig. 13A)
528 while overexpression of Ptc2 by placing the *GALI* promoter in front of the chromosomal
529 *PTC2* gene had no effect of growth of ER-stressed cells (data not shown). Overexpression of
530 WT Dcr2 and catalytically inactive H338A-Dcr2 (63) from the *GALI* promoter on a 2 μ
531 plasmid inhibited growth of unstressed WT cells to the same extent, but did not affect
532 survival of ER stress (Fig. 13C). Deletion of *IRE1* slightly impaired growth on raffinose and
533 galactose (Fig. 13C) and largely masked the negative effects of expression of WT and
534 H338A-Dcr2 on growth of unstressed cells (Fig. 13C). Expression of WT or H338A-Dcr2 did
535 not alter survival of ER stress by *ire1* Δ cells (Fig. 13C). These data suggest that
536 overexpression of Dcr2 does not affect survival of ER stress.

537 To characterise whether deletion of *DCR2* or *PTC2* affects survival of ER stress we
538 constructed *dcr2* Δ and *ptc2* Δ strains, and double *dcr2* Δ *ptc2* Δ strains. Survival of ER stress
539 was not altered by deletion of *DCR2*, deletion of *PTC2*, or by simultaneous deletion of both
540 *DCR2* and *PTC2* (Fig. 13D). These data suggest that negative regulation of Ire1 by Dcr2 and
541 Ptc2 to optimally tune the amplitude of the Ire1 signalling output is not required to survive
542 ER stress or that other phosphatases exist that can compensate for the loss of both Dcr2 and
543 Ptc2 in *dcr2* Δ *ptc2* Δ cells.

544 **Discussion**

545 The data presented here show that Ire1 can transduce a partial ER stress signal in the absence
546 of phosphorylation in its activation loop (Figs. 3 and 4). The partial activation of *HAC1*
547 splicing by activation loop mutants resulted in partial induction of *KAR2* and *PDII* mRNAs
548 (Fig. 3D, E) and partial protection from ER stress (Fig. 6). In addition, we show that
549 transduction of this partial ER stress signal by activation loop mutants relies on the presence

550 of a negatively charged amino acid such as an aspartate or a glutamate in the activation loop,
551 which has been conserved throughout evolution in fungal and plant Ire1 (Fig. 1). Mutation of
552 this aspartate, D836 in *S. cerevisiae* Ire1, to alanine in activation loop mutants nearly
553 completely eliminated production of *HAC1ⁱ* mRNA, induction of *KAR2* and *PDII* mRNA, of
554 an UPRE-*lacZ* reporter, and survival of ER stress (Figs. 8, 9 and 11). In this way,
555 introduction of the D836A mutation into activation loop mutants is reminiscent of the *in vitro*
556 behaviour of human IRE1 α . IRE1 α lacks negatively charged amino acids in its activation
557 loop (Fig. 1A) and displayed a ~100-fold increase of its V_{\max} and k_{cat} upon phosphorylation
558 (22). By contrast, the D836A mutation by itself had no effect, because the levels of *HAC1*
559 splicing, induction of *KAR2* and *PDII* mRNA and of the UPRE-*lacZ* reporter, and survival of
560 ER stress were indistinguishable from cells expressing WT Ire1. These observations suggest
561 that D836 can partially substitute for activation loop phosphorylation in the activation loop
562 mutants.

563 The role of activation loop phosphorylation in activation of Ire1 is thought to lie in
564 conformational changes in the activation loop that result in opening of the ATP binding
565 pocket (18). Binding of ATP then induces oligomerisation of Ire1 and RNase activity (18). In
566 this model for activation of Ire1, point mutations in the protein kinase domain, that largely
567 inactivate the protein kinase activity of Ire1, should display a significant loss of RNase
568 activity. However, mutation of D828, which contributes to coordinating two Mg²⁺ ions
569 important for catalysis of the γ -phosphoryl transfer reaction, or mutation of the catalytic
570 aspartate, D797, did not destroy RNase activity (7, 21). Retention of RNase activity by these
571 protein kinase mutants may, as in the case for the activation loop mutants, be explained by
572 the presence of D836 in the activation loop.

573 Based on its primary amino acid sequence, Ire1 belongs to the family of RD kinases and
574 its reliance on activation loop phosphorylation for full activity [Figs. 2 and 3 and (22)]

575 suggests that Ire1 belongs to the family of phosphorylation-dependent RD protein kinases. In
576 these protein kinases phosphoamino acids in the activation loop move into a basic pocket
577 formed by the invariant arginine that precedes the catalytic aspartate (R796 in *S. cerevisiae*
578 Ire1) and a second basic amino acid located in strand β 9 (K833 on strand β 10 in Ire1). The
579 crystal structure of oligomeric Ire1 shows phosphorylated T844 in contact with this basic
580 pocket (4), as would be expected for a phosphorylation-dependent RD kinase. However,
581 phosphorylation at T844 is of lesser importance than phosphorylation at S840 or S841,
582 because induction of both *KAR2* and *PDII* mRNAs was more severely affected in the S840A
583 S841A double mutant than the T844A single mutant (3). The importance of S840 or S841 in
584 activation of Ire1 is further supported by the observation that all phosphorylation site mutants
585 show a similar decrease in *HAC1* splicing and induction of both *KAR2* and *PDII* (Fig. 3).
586 This suggests that the other phosphorylation sites may only play minor roles or require the
587 presence of S840 or S841 to mediate activation of the endoribonuclease domain. Data
588 obtained from the β -galactosidase reporter assays (Fig. 4) indicate that the other
589 phosphorylation sites can mediate some activation of the endoribonuclease domain
590 independent of S840 or S841. Introduction of the D836A mutation into any of the three
591 phosphorylation site mutants nearly completely abolished *HAC1* splicing, induction of *KAR2*,
592 *PDII*, and the β -galactosidase reporter, and survival of ER stress (Figs. 8, 9, and 11). This
593 behaviour of the D836A mutation suggests that the residual ER stress response transduced by
594 S840A-S841A-Ire1 relies on D836 and that D836 can partially substitute for functions
595 provided by S840 or S841 in WT Ire1. In the absence of D836, S840 and S841 the other
596 phosphorylation sites can no longer mediate effective activation of Ire1 (Figs. 8, 9, and 11),
597 which suggests that a function provided by D836, S840 or S841 is necessary for activation of
598 Ire1. At the same time, induction of the β -galactosidase reporter decreases from S840A-
599 S841A-Ire1, to Q-A-Ire1, and P-A-Ire1 (Fig. 4), which suggests that the ability of D836 to

600 mediate activation of Ire1 requires at least one of the other phosphorylation sites. These data
601 are consistent with the view that the activation loop makes at least two contacts necessary for
602 activation of Ire1, one mediated by S840 or S841, and in their absence, and to a lesser degree,
603 by D836, and a second one mediated by one of the other phosphorylation sites.

604 The crystal structure of oligomeric Ire1 suggests that two contacts of the activation loop
605 necessary for activation of Ire1 are made between phosphorylated S840 and S841 and R896
606 of the same molecule and K678 of an adjacent Ire1 molecule, and between phosphorylated
607 T844 and the RD pocket (4). D836 may simply substitute for S840 and S841 by contacting
608 the same basic pocket, while phosphorylated T844 still remains in contact with the RD
609 pocket, but it is also possible that D836 contacts the RD pocket and that phosphorylated
610 T844, phosphorylated S837, or phosphorylated S850 contact the basic pocket formed by
611 R896 and K678 in S840A S841A mutants. Contacts made between the phosphorylated
612 activation loop and basic pockets have been proposed to facilitate oligomerisation of Ire1 (4).
613 *In vivo* clustering of Ire1, however, was not affected by the activation loop mutants (Fig. 5) or
614 by introduction of the D836A mutation into any of the activation loop mutants (Fig. 10).
615 These observations suggest that surfaces other than the phosphorylated activation loop suffice
616 to mediate efficient clustering of Ire1 *in vivo*. Therefore, it seems that the critical roles of
617 activation loop phosphorylation in activation of Ire1 may not lie in facilitating clustering of
618 Ire1.

619 D836 can only partially substitute for phosphorylation of S840 or S841, because all
620 activation loop mutants can only support levels of *HAC1* splicing that are significantly lower
621 than in cells expressing WT Ire1. This may be due to the decreased negative charge of a
622 carboxylate when compared to a phosphate and subsequent partial neutralisation of positive
623 charges in basic pockets, such as the basic pocket formed by R896 and K678 of an adjacent
624 Ire1 molecule, resulting in decreased stability of active conformations. In addition, steric

625 constraints may prevent the smaller aspartate to move as close to positive charges as
626 phosphoamino acids might, which again may destabilise active conformations. Furthermore,
627 D836 can only make one contact to basic pockets, whereas, for example, phosphorylated
628 S840 and S841 can make two contacts to the same basic pocket (4). The lack of a phenotype
629 for cells expressing D836A-Ire1 suggests that conformations formed by phosphorylated Ire1
630 are more stable or longer-lived than any conformations in which D836 attempts to take over
631 any roles of phosphorylation. Alternatively, phosphorylation may be kinetically
632 outcompeting formation of any conformations in which D836 replaces phosphoserines or
633 phosphothreonines.

634 Inactivation of Ire1 is thought to involve its dephosphorylation (21, 22), but also its
635 autophosphorylation in its α EF insertion loop (7, 21). The similar inactivation kinetics of WT
636 Ire1 and activation loop mutants (Fig. 12) suggests that inactivation of Ire1 is a twostep
637 process in which fast dephosphorylation of Ire1 precedes slower, phosphorylation-
638 independent steps (Fig. 12). In the DTT wash-out experiments (Fig. 12) only the slower
639 phosphorylation-independent steps may have been observed. These phosphorylation-
640 independent steps may represent the reassociation of Kar2 with the luminal domain of Ire1
641 (64-67), the disassembly of Ire1 oligomers, or the clearance of misfolded and damaged
642 proteins from the ER via ER-associated degradation or dilution by growth. We observed no
643 noticeable differences in the disassembly of Ire1 foci in cells expressing WT Ire1,
644 phosphorylation site mutants (Fig. 5), or a combination of phosphorylation site mutants and
645 the D836A mutation (Fig. 10). Thus, while activation of Ire1 leading to *HAC1* splicing
646 requires at least one negative charge in the activation loop, inactivation of Ire1 and
647 dissolution of Ire1 clusters proceeds independent of negative charges on the activation loop.

648 The initial, fast dephosphorylation in the inactivation of Ire1 may be mediated by the
649 phosphatases Dcr2 (30) or Ptc2 (31). Overexpression of Ptc2 in cells expressing different

650 *IRE1* alleles revealed that deletion of *IRE1* or expression of *IRE1* alleles that lack all potential
651 phosphorylation sites mask the effects of overexpression of Ptc2 (Fig. 13A). These findings
652 are consistent with the view that Ptc2 may attenuate Ire1 signalling by dephosphorylating the
653 activation loop of Ire1, resulting in decreased levels of *HAC1* splicing (31). However,
654 decreased phosphorylation of the activation loop in activation loop mutants may impair ATP
655 binding (18) and decrease the protein kinase activity of Ire1 leading to decreased
656 phosphorylation of other regions of Ire1 such as its α EF insertion loop. Therefore, the
657 epistatic relationship between Ire1 and Ptc2 may also be explained by dephosphorylation of
658 regions other than the activation loop by Ptc2. In contrast to Ptc2, we found no evidence that
659 overexpression of Dcr2 affects survival of ER stress (Fig. 13B, C). We also do not observe a
660 synthetic growth defect in *ire1 Δ dcr2 Δ* cells (Fig. 13D) or that deletion of *DCR2* impairs
661 survival of ER stress which contrasts to previously reported results (30). While these different
662 results may be explained by the different genetic backgrounds, W303 and S288c, used in the
663 two studies, we also did not observe any effects of overexpression of Dcr2 from the *GALI*
664 promoter on the 2 μ plasmid pRS425 in the S288c genetic background (data not shown).

665 Deletion of *IRE1* or expression of D836A-P-A-Ire1 also masks the toxic effects of
666 overexpression of WT and catalytically inactive Ptc2 and Dcr2 on growth of unstressed cells
667 (Fig. 13A, C). For *PTC2* similar epistatic relationships to *IRE1* seem to exist in unstressed
668 and ER-stressed cells, suggesting that Ptc2 may act through the same mechanism in
669 unstressed and ER-stressed cells. It is unlikely that unmasking of the inositol auxotrophy of
670 *ire1 Δ* cells (68) by overexpression of Ptc2 can explain the growth inhibitory effects of Ptc2,
671 because increasing the inositol concentration did not mitigate the growth inhibitory effects of
672 overexpression of Ptc2 (data not shown). Deletion of *IRE1* is also epistatic to overexpression
673 of Dcr2 in unstressed cells (Fig. 13C). The lack of any effect of overexpression of *DCR2* on
674 growth in the presence of ER stress suggests another genetic relationship between *IRE1* and

675 *DCR2* than between *IRE1* and *PTC2*. Deletion of *IRE1* may, for example, perturb a secretory
676 pathway function that is located upstream of a secretory pathway function of Dcr2.

677 In summary, our work shows that yeast Ire1 retains the ability to transduce a weak ER
678 stress signal when all its phosphorylation sites in its activation have been mutated to alanine.
679 The ability of these activation loop mutants to respond to ER stress relies on the presence of a
680 negatively charged amino acid in the activation loop. These findings provide a molecular
681 explanation for some of the differences between yeast and mammalian Ire1.

682 **Acknowledgements**

683 We thank P. Walter (University of California at San Francisco, San Francisco, CA, USA) for
684 providing plasmids YCplac33-*IRE1*-HA, YCplac33-L745A-*IRE1*-HA, and YCplac33-
685 S840A-S841A-*IRE1*-HA and yeast strain PWY 260, T. Dever (National Institute of Child
686 Health and Human Development, National Institutes of Health, Bethesda, MD, USA) for
687 providing plasmid pC3060-S840A-S841A-T844A-S850A, and W. A. Prinz for providing
688 plasmid pJK59. We thank J. Robson and T. Hawkins for help with the confocal microscopy
689 and C. Beeby, R. Berrisford, O. Graham, S. Ohanees, and B. Wattam for technical help.

690 **Funding information**

691 This work was supported by the Biotechnology and Biological Sciences Research Council
692 [BB/D01588X/1] and the Scientific Grant Agency of the Ministry of Education of the Slovak
693 Republic and the Slovak Academy of Sciences, the project VEGA 02/0188/14. The North
694 East Proteome Analysis Facility (NEPAF) was funded by ONE North East and the European
695 Development Fund. The funders had no role in study design, data collection and
696 interpretation, or the decision to submit the work for publication.

697 **Author contributions**

698 MCA, SS, AAA, AT, and MS designed the experiments and analysed the data. MCA, SS,
699 AAA, HAMS, MB, KB, and MS performed the experiments. MS devised the study and wrote

700 the manuscript. All authors read and approved of the manuscript. The authors declare no
701 competing or financial interests.

702 **References**

- 703
- 704 1. **Cox JS, Shamu CE, Walter P.** 1993. Transcriptional induction of genes encoding
705 endoplasmic reticulum resident proteins requires a transmembrane protein kinase. *Cell*
706 **73**:1197-1206.
- 707 2. **Mori K, Ma W, Gething M-J, Sambrook J.** 1993. A transmembrane protein with a
708 *cdc2⁺/CDC28*-related kinase activity is required for signaling from the ER to the nucleus.
709 *Cell* **74**:743-756.
- 710 3. **Shamu CE, Walter P.** 1996. Oligomerization and phosphorylation of the Ire1p kinase
711 during intracellular signaling from the endoplasmic reticulum to the nucleus. *EMBO J*
712 **15**:3028-3039.
- 713 4. **Korennykh AV, Egea PF, Korostelev AA, Finer-Moore J, Zhang C, Shokat KM,**
714 **Stroud RM, Walter P.** 2009. The unfolded protein response signals through high-order
715 assembly of Ire1. *Nature* **457**:687-693.
- 716 5. **Aragón T, van Anken E, Pincus D, Serafimova IM, Korennykh AV, Rubio CA,**
717 **Walter P.** 2008. Messenger RNA targeting to endoplasmic reticulum stress signalling
718 sites. *Nature* **457**:736-740.
- 719 6. **Kimata Y.** 2008. [Mechanisms of sensing endoplasmic reticulum stress]. *Tanpakushitsu*
720 *Kakusan Koso* **53**:12-19.
- 721 7. **Rubio C, Pincus D, Korennykh A, Schuck S, El-Samad H, Walter P.** 2011.
722 Homeostatic adaptation to endoplasmic reticulum stress depends on Ire1 kinase activity. *J*
723 *Cell Biol* **193**:171-184.
- 724 8. **Cox JS, Walter P.** 1996. A novel mechanism for regulating activity of a transcription
725 factor that controls the unfolded protein response. *Cell* **87**:391-404.

- 726 9. **Sidrauski C, Walter P.** 1997. The transmembrane kinase Ire1p is a site-specific
727 endonuclease that initiates mRNA splicing in the unfolded protein response. *Cell*
728 **90**:1031-1039.
- 729 10. **Kawahara T, Yanagi H, Yura T, Mori K.** 1997. Endoplasmic reticulum stress-induced
730 mRNA splicing permits synthesis of transcription factor Hac1p/Ern4p that activates the
731 unfolded protein response. *Mol Biol Cell* **8**:1845-1862.
- 732 11. **Kawahara T, Yanagi H, Yura T, Mori K.** 1998. Unconventional splicing of
733 *HAC1/ERN4* mRNA required for the unfolded protein response. Sequence-specific and
734 non-sequential cleavage of the splice sites. *J Biol Chem* **273**:1802-1807.
- 735 12. **Rüegsegger U, Leber JH, Walter P.** 2001. Block of *HAC1* mRNA translation by long-
736 range base pairing is released by cytoplasmic splicing upon induction of the unfolded
737 protein response. *Cell* **107**:103-114.
- 738 13. **Sidrauski C, Cox JS, Walter P.** 1996. tRNA ligase is required for regulated mRNA
739 splicing in the unfolded protein response. *Cell* **87**:405-413.
- 740 14. **Mori K, Sant A, Kohno K, Normington K, Gething MJ, Sambrook JF.** 1992. A 22 bp
741 cis-acting element is necessary and sufficient for the induction of the yeast *KAR2* (BiP)
742 gene by unfolded proteins. *EMBO J* **11**:2583-2593.
- 743 15. **Kohno K, Normington K, Sambrook J, Gething MJ, Mori K.** 1993. The promoter
744 region of the yeast *KAR2* (BiP) gene contains a regulatory domain that responds to the
745 presence of unfolded proteins in the endoplasmic reticulum. *Mol Cell Biol* **13**:877-890.
- 746 16. **Mori K, Ogawa N, Kawahara T, Yanagi H, Yura T.** 1998. Palindrome with spacer of
747 one nucleotide is characteristic of the *cis*-acting unfolded protein response element in
748 *Saccharomyces cerevisiae*. *J Biol Chem* **273**:9912-9920.
- 749 17. **Leber JH, Bernales S, Walter P.** 2004. *IRE1*-independent gain control of the unfolded
750 protein response. *PLoS Biol* **2**:1197-1207.

- 751 18. **Lee KP, Dey M, Neculai D, Cao C, Dever TE, Sicheri F.** 2008. Structure of the dual
752 enzyme Ire1 reveals the basis for catalysis and regulation in nonconventional RNA
753 splicing. *Cell* **132**:89-100.
- 754 19. **Nolen B, Taylor S, Ghosh G.** 2004. Regulation of protein kinases; controlling activity
755 through activation segment conformation. *Mol Cell* **15**:661-675.
- 756 20. **Johnson LN, Noble MEM, Owen DJ.** 1996. Active and inactive protein kinases:
757 Structural basis for regulation. *Cell* **85**:149-158.
- 758 21. **Chawla A, Chakrabarti S, Ghosh G, Niwa M.** 2011. Attenuation of yeast UPR is
759 essential for survival and is mediated by IRE1 kinase. *J Cell Biol* **191**:41-50.
- 760 22. **Prischi F, Nowak PR, Carrara M, Ali MM.** 2014. Phosphoregulation of Ire1 RNase
761 splicing activity. *Nat Commun* **5**:3554.
- 762 23. **Papa FR, Zhang C, Shokat K, Walter P.** 2003. Bypassing a kinase activity with an
763 ATP-competitive drug. *Science* **302**:1533-1537.
- 764 24. **Prinz WA, Grzyb L, Veenhuis M, Kahana JA, Silver PA, Rapoport TA.** 2000.
765 Mutants affecting the structure of the cortical endoplasmic reticulum in *Saccharomyces*
766 *cerevisiae*. *J Cell Biol* **150**:461-474.
- 767 25. **Vieira J, Messing J.** 1982. The pUC plasmids, an M13mp7-derived system for insertion
768 mutagenesis and sequencing with synthetic universal primers. *Gene* **19**:259-268.
- 769 26. **Welihinda AA, Kaufman RJ.** 1996. The unfolded protein response pathway in
770 *Saccharomyces cerevisiae*. Oligomerization and trans-phosphorylation of Ire1p (Ern1p)
771 are required for kinase activation. *J Biol Chem* **271**:18181-18187.
- 772 27. **Gelperin DM, White MA, Wilkinson ML, Kon Y, Kung LA, Wise KJ, Lopez-Hoyo**
773 **N, Jiang L, Piccirillo S, Yu H, Gerstein M, Dumont ME, Phizicky EM, Snyder M,**
774 **Grayhack EJ.** 2005. Biochemical and genetic analysis of the yeast proteome with a
775 movable ORF collection. *Genes Dev* **19**:2816-2826.

- 776 28. **Chee MK, Haase SB.** 2012. New and redesigned pRS plasmid shuttle vectors for genetic
777 manipulation of *Saccharomyces cerevisiae*. *G3 (Bethesda)* **2**:515-526.
- 778 29. **Christianson TW, Sikorski RS, Dante M, Shero JH, Hieter P.** 1992. Multifunctional
779 yeast high-copy-number shuttle vectors. *Gene* **110**:119-122.
- 780 30. **Guo J, Polymenis M.** 2006. Dcr2 targets Ire1 and downregulates the unfolded protein
781 response in *Saccharomyces cerevisiae*. *EMBO Rep* **7**:1124-1127.
- 782 31. **Welihinda AA, Tirasophon W, Green SR, Kaufman RJ.** 1998. Protein serine/threonine
783 phosphatase Ptc2p negatively regulates the unfolded-protein response by
784 dephosphorylating Ire1p kinase. *Mol Cell Biol* **18**:1967-1977.
- 785 32. **Chen D-C, Yang B-C, Kuo T-T.** 1992. One-step transformation of yeast in stationary
786 phase. *Curr Genet* **21**:83-84.
- 787 33. **Rothstein RJ.** 1983. One-step gene disruption in yeast. *Methods Enzymol* **101**:202-211.
- 788 34. **Schröder M, Chang JS, Kaufman RJ.** 2000. The unfolded protein response represses
789 nitrogen-starvation induced developmental differentiation in yeast. *Genes Dev* **14**:2962-
790 2975.
- 791 35. **Wach A, Brachat A, Pöhlmann R, Philippsen P.** 1994. New heterologous modules for
792 classical or PCR-based gene disruptions in *Saccharomyces cerevisiae*. *Yeast* **10**:1793-
793 1808.
- 794 36. **Janke C, Magiera MM, Rathfelder N, Taxis C, Reber S, Maekawa H, Moreno-
795 Borchart A, Doenges G, Schwob E, Schiebel E, Knop M.** 2004. A versatile toolbox for
796 PCR-based tagging of yeast genes: new fluorescent proteins, more markers and promoter
797 substitution cassettes. *Yeast* **21**:947-962.
- 798 37. **Longtine MS, McKenzie A, 3rd, Demarini DJ, Shah NG, Wach A, Brachat A,
799 Philippsen P, Pringle JR.** 1998. Additional modules for versatile and economical PCR-
800 based gene deletion and modification in *Saccharomyces cerevisiae*. *Yeast* **14**:953-961.

- 801 38. **Sherman F.** 1991. Getting started with yeast. *Methods Enzymol* **194**:3-21.
- 802 39. **Schröder M, Clark R, Kaufman RJ.** 2003. *IRE1-* and *HAC1*-independent
803 transcriptional regulation in the unfolded protein response of yeast. *Mol Microbiol*
804 **49**:591-606.
- 805 40. **Law DT, Segall J.** 1988. The *SPS100* gene of *Saccharomyces cerevisiae* is activated late
806 in the sporulation process and contributes to spore wall maturation. *Mol Cell Biol* **8**:912-
807 922.
- 808 41. **Smith PK, Krohn RI, Hermanson GT, Mallia AK, Gartner FH, Provenzano MD,**
809 **Fujimoto EK, Goeke NM, Olson BJ, Klenk DC.** 1985. Measurement of protein using
810 bicinchoninic acid. *Anal Biochem* **150**:76-85.
- 811 42. **Laemmli UK.** 1970. Cleavage of structural proteins during the assembly of the head of
812 bacteriophage T4. *Nature* **227**:680-685.
- 813 43. **Schröder M, Friedl P.** 1997. Overexpression of recombinant human antithrombin III in
814 Chinese hamster ovary cells results in malformation and decreased secretion of the
815 recombinant protein. *Biotechnol Bioeng* **53**:547-559.
- 816 44. **Studier FW.** 2005. Protein production by auto-induction in high density shaking cultures.
817 *Protein Expr Purif* **41**:207-234.
- 818 45. **Maltman DJ, Simon WJ, Wheeler CH, Dunn MJ, Wait R, Slabas AR.** 2002.
819 Proteomic analysis of the endoplasmic reticulum from developing and germinating seed
820 of castor (*Ricinus communis*). *Electrophoresis* **23**:626-639.
- 821 46. **Olsen JV, de Godoy LMF, Li G, Macek B, Mortensen P, Pesch R, Makarov A,**
822 **Lange O, Horning S, Mann M.** 2005. Parts per million mass accuracy on an Orbitrap
823 mass spectrometer via lock mass injection into a C-trap. *Mol Cell Proteomics* **4**:2010-
824 2021.

- 825 47. **Amacher DE**. 2011. The mechanistic basis for the induction of hepatic steatosis by
826 xenobiotics. *Expert Opin Drug Metab Toxicol* doi:10.1517/17425255.2011.577740.
- 827 48. **Vizcaino JA, Csordas A, del-Toro N, Dianas JA, Griss J, Lavidas I, Mayer G, Perez-**
828 **Riverol Y, Reisinger F, Ternent T, Xu QW, Wang R, Hermjakob H**. 2016. 2016
829 update of the PRIDE database and its related tools. *Nucleic Acids Res* **44**:D447-456.
- 830 49. **Ku HH**. 1966. Notes on the use of propagation of error formulas. *J Res Nat Bureau*
831 *Standards Sect C - Eng Instrumentat* **70**:263-273.
- 832 50. **D'Agostino R, Pearson ES**. 1973. Tests for departure from normality. Empirical results
833 for the distributions of b_2 and $\sqrt{b_1}$. *Biometrika* **60**:613-622.
- 834 51. **Brown MB, Forsythe AB**. 1974. Robust tests for the equality of variances. *J Am Stat*
835 *Assoc* **69**:364-367.
- 836 52. **Bartlett MS**. 1937. Properties of sufficiency and statistical tests. *Proc Royal Soc Lond*
837 *Ser A Math Phys Sci* **160**:268-282.
- 838 53. **Little TM, Hills FJ**. 1972. *Statistical Methods in Agricultural Research*. University of
839 California Agricultural Extension, Davis.
- 840 54. **Tukey JW**. 1949. One degree of freedom for non-additivity. *Biometrics* **5**:232-242.
- 841 55. **Welch BL**. 1947. The generalisation of student's problems when several different
842 population variances are involved. *Biometrika* **34**:28-35.
- 843 56. **Games PA, Howell JF**. 1976. Pairwise multiple comparison procedures with unequal N's
844 and/or variances: A Monte Carlo study. *J Educ Stat* **1**:113-125.
- 845 57. **Bishop AC, Shah K, Liu Y, Witucki L, Kung C, Shokat KM**. 1998. Design of allele-
846 specific inhibitors to probe protein kinase signaling. *Curr Biol* **8**:257-266.
- 847 58. **Bishop AC, Ubersax JA, Petsch DT, Matheos DP, Gray NS, Blethrow J, Shimizu E,**
848 **Tsien JZ, Schultz PG, Rose MD, Wood JL, Morgan DO, Shokat KM**. 2000. A
849 chemical switch for inhibitor-sensitive alleles of any protein kinase. *Nature* **407**:395-401.

- 850 59. **Bachmair A, Finley D, Varshavsky A.** 1986. In vivo half-life of a protein is a function
851 of its amino-terminal residue. *Science* **234**:179-186.
- 852 60. **Owen DJ, Noble MEM, Garman EF, Papageorgiou AC, Johnson LN.** 1995. Two
853 structures of the catalytic domain of phosphorylase kinase: an active protein kinase
854 complexed with substrate analogue and product. *Structure* **3**:467-482.
- 855 61. **Skamnaki VT, Owen DJ, Noble ME, Lowe ED, Lowe G, Oikonomakos NG, Johnson**
856 **LN.** 1999. Catalytic mechanism of phosphorylase kinase probed by mutational studies.
857 *Biochemistry* **38**:14718-14730.
- 858 62. **Jeffrey PD, Russo AA, Polyak K, Gibbs E, Hurwitz J, Massagué J, Pavletich NP.**
859 1995. Mechanism of CDK activation revealed by the structure of a cyclinA-CDK2
860 complex. *Nature* **376**:313-320.
- 861 63. **Pathak R, Bogomolnaya LM, Guo J, Polymenis M.** 2004. Gid8p (Dcr1p) and Dcr2p
862 function in a common pathway to promote START completion in *Saccharomyces*
863 *cerevisiae*. *Eukaryot Cell* **3**:1627-1638.
- 864 64. **Pincus D, Chevalier MW, Aragón T, van Anken E, Vidal SE, El-Samad H, Walter P.**
865 2010. BiP binding to the ER-stress sensor Ire1 tunes the homeostatic behavior of the
866 unfolded protein response. *PLoS Biol* **8**:e1000415.
- 867 65. **Bertolotti A, Zhang Y, Hendershot LM, Harding HP, Ron D.** 2000. Dynamic
868 interaction of BiP and ER stress transducers in the unfolded-protein response. *Nat Cell*
869 *Biol* **2**:326-332.
- 870 66. **Okamura K, Kimata Y, Higashio H, Tsuru A, Kohno K.** 2000. Dissociation of
871 Kar2p/BiP from an ER sensory molecule, Ire1p, triggers the unfolded protein response in
872 yeast. *Biochem Biophys Res Commun* **279**:445-450.

- 873 67. **Kimata Y, Kimata YI, Shimizu Y, Abe H, Farcasanu IC, Takeuchi M, Rose MD,**
 874 **Kohno K.** 2003. Genetic evidence for a role of BiP/Kar2 that regulates Ire1 in response to
 875 accumulation of unfolded proteins. *Mol Biol Cell* **14**:2559-2569.
- 876 68. **Nikawa J, Yamashita S.** 1992. *IRE1* encodes a putative protein kinase containing a
 877 membrane-spanning domain and is required for inositol phototrophy in *Saccharomyces*
 878 *cerevisiae*. *Mol Microbiol* **6**:1441-1446.
- 879 69. **Tukey JW.** 1949. Comparing individual means in the analysis of variance. *Biometrics*
 880 **5**:99-114.
- 881 70. **Winzeler EA, Richards DR, Conway AR, Goldstein AL, Kalman S, McCullough MJ,**
 882 **McCusker JH, Stevens DA, Wodicka L, Lockhart DJ, Davis RW.** 1998. Direct allelic
 883 variation scanning of the yeast genome. *Science* **281**:1194-1197.

884 **Figure legends**

885 **Figure 1. Sequence alignment of the activation segment of Ire1.** The GenBank accession
 886 numbers are: *Arabidopsis thaliana* 1 - NP_568444, *A. thaliana* 2 - NP_565419, *Ashbya*
 887 *gossypii* - NP_984389, *Aspergillus fumigatus* - XP_749922, *Caenorhabditis elegans* -
 888 AAL30828, *Candida albicans* - XP_717532, *Drosophila melanogaster* - NP_001097839,
 889 *Homo sapiens* α - NP_001424; *H. sapiens* β - NP_150296, *Saccharomyces cerevisiae* -
 890 NP_011946, and *Trichoderma reesei* - AAP92915. The sequence for *Saccharomyces bayanus*
 891 Ire1 was obtained from the *Saccharomyces genome* database. Amino acids in the activation
 892 loop are shown in blue, potential phosphoacceptor sites in red, and aspartic and glutamic acid
 893 in orange.

894 **Figure 2. Ire1 autophosphorylates at S837.** (A) Fragmentation spectrum 1976 for the
 895 peptide 835 LDSGQpSpSFRTNLNNPpSGTSGWR 856 derived from WT Ire1. Detected mass to
 896 charge ratios for the $^{+1}$ y (red) and $^{+2}$ y (blue) ion series are shown. Brackets highlight
 897 fragmentations that are explained by the presence of phosphoryl groups. The difference

898 between the observed mass to charge ratio and the monoisotopic mass to charge ratio for the
 899 unphosphorylated ions are indicated. **(B)** Fragmentation spectrum 2031 for the peptide
 900 ⁸³⁵LDSGQpSSFRpTNLNNPpSGTSGWR⁸⁵⁶ derived from WT Ire1. **(C)** Fragmentation
 901 spectrum 1462 for the peptide ⁸³⁴KLDpSGQp(SS)FRpTNLNNPp(SGTS)GWR⁸⁵⁶ derived
 902 from L745A-Ire1. Detected mass to charge ratios for the ⁺¹y (red) and ⁺¹b (oranges) ion series
 903 are shown. In addition, one phosphoryl group is bound to S840 or S841, another phosphoryl
 904 group to S850, T852, or S853.

905 **Figure 3. Mutation of phosphorylation sites in the activation loop decreases, but does**
 906 **not abolish, cleavage of *HAC1* mRNA by Ire1.** **(A)** Northern blots for *HAC1*, *KAR2*, *PDII*,
 907 and the loading control pC4/2 (40) on RNA extracted from *ire1Δ* strains expressing the
 908 indicated *IRE1* alleles from YCplac33 or carrying empty vector ('-'). Mid-exponential growth
 909 phase cells were treated with 2 mM DTT for the indicated times. Abbreviations: *HAC1*^u -
 910 unspliced *HAC1* mRNA, *HAC1*ⁱ - spliced *HAC1* mRNA, 1st + i. - 1st exon of *HAC1*^u mRNA
 911 plus the intron, and 1st - 1st exon of *HAC1*^u mRNA. **(B)** Quantification and 95% (open
 912 symbols), 99% (half-filled symbols), or 99.9% (filled symbols) confidence intervals of the
 913 percentage of *HAC1*ⁱ mRNA (% *HAC1*ⁱ), **(C)** the percentage of *HAC1* mRNA cleavage (%
 914 Cleavage), **(D)** induction of *KAR2* and of **(E)** *PDII* mRNAs. Bars represent the standard error
 915 ($n = 8$ for the WT, $n = 5$ for all other strains). The confidence intervals for % *HAC1*ⁱ, %
 916 cleavage, ln-transformed *KAR2* and *PDII* mRNA levels were calculated using an ordinary
 917 two-way ANOVA with Tukey's correction for multiple comparisons (69). Abbreviations: 2S-
 918 A = S840-A S841A, P-A = S837A S840A S841A T844A S850A and Q-A = S840A S841A
 919 T844A S850A.

920 **Figure 4. Mutation of all phosphorylation sites in the activation loop decreases, but does**
 921 **not abolish, induction of UPRE-*lacZ* reporters.** **(A)** β -Galactosidase activity standardised
 922 to total cellular protein before, 1 h, and 2 h after induction of ER stress with 2 mM DTT in

923 mid-exponential *ire1Δ* cells expressing the indicated *IRE1* alleles from YCplac33 or carrying
924 empty vector ('-'). Bars represent standard errors ($n = 3$ for all strains). **(B)** 95% (open
925 symbols), 99% (half-filled symbols), or 99.9% (filled symbols) confidence intervals (CI)
926 were calculated for the ln-transformed data with an ordinary two-way ANOVA with Tukey's
927 correction for multiple comparisons.

928 **Figure 5. Activation loop phosphorylation is dispensable for clustering of Ire1 *in vivo*.**

929 Location of Sec63-GFP and Ire1-mCherry in unstressed cells and cells exposed to 2 mM
930 DTT for 15 min, 1 h or after wash out of DTT for 1 h from cells treated with 2 mM DTT for
931 2 h. Sec63-GFP was expressed from the single copy *URA3* plasmid pJK59 in *ire1Δ* cells
932 transformed with single copy *LEU2* plasmids derived from pEvA97 that carry the indicated
933 *IRE1* alleles. Images covering ~100 cells were taken, except for the DTT wash out
934 experiment in which ~20 cells were analysed. Representative images are shown. Scale bar – 5
935 μm .

936 **Figure 6. Survival of ER stress by activation loop mutants.** Survival of ER stress induced

937 with 0.4 and 0.8 $\mu\text{g/ml}$ tunicamycin (Tm). Serial 10-fold dilutions of fresh overnight cultures
938 of *ire1Δ* cells expressing the indicated *IRE1* alleles from YCplac33 or carrying empty vector
939 ('-') were spotted on SD minus uracil plates containing 0.4 or 0.8 $\mu\text{g/ml}$ Tm and allowed to
940 grow for 2-3 d before taking photographs. #1 and #2 indicate two independent transformants
941 for the S840A S841A and Q-A mutants. The experiment was repeated three times with
942 qualitatively similar results.

943 **Figure 7. Expression of WT and mutant Ire1 proteins.** **(A)** Western blots for HA-tagged

944 Ire1 and Act1 isolated from mid-exponential growth phase *ire1Δ* strains expressing the
945 indicated *IRE1* alleles from YCplac33 or carrying empty vector ('-'). Cells were treated for 2
946 h with 2 mM DTT where indicated ('+'). PVDF membranes were stained with Ponceau S
947 after electrotransfer of proteins from 8% SDS-PAGE gels. **(B)** Quantification of Ire1-HA

948 levels relative to the Act1 loading control. The expression level of Ire1-HA in untreated WT
 949 cells was arbitrarily set to 1.0. The data were analysed with an ordinary two-way ANOVA
 950 with Tukey's correction for multiple comparisons. No significant differences in Ire1-HA
 951 expression levels were detected, except for the negative control strain transformed with
 952 empty vector. Bars represent standard errors ($n = 7$ for the WT, $n = 4$ for the Q-A, D836A Q-
 953 A, P-A, and D836A P-A mutants, and $n = 3$ for the D836A, S840A S841A, and D836A
 954 S840A S841A mutants and the strain transformed with empty vector).

955 **Figure 8. D836 is required for cleavage of *HAC1* mRNA by activation loop mutants. (A)**

956 Northern blots for *HAC1*, *KAR2*, *PDII*, and the loading control pC4/2 (40) on RNA extracted
 957 from *ire1Δ* strains expressing the indicated *IRE1* alleles from YCplac33 or carrying empty
 958 vector ('-'). Mid-exponential growth phase cells were treated with 2 mM DTT for the
 959 indicated times. **(B)** Quantification of the percentage of *HAC1*ⁱ mRNA (% *HAC1*ⁱ), **(C)** the
 960 percentage of *HAC1* mRNA cleavage (% Cleavage), **(D)** induction of *KAR2* and of **(E)** *PDII*
 961 mRNAs. Bars represent standard errors. * - $P \leq 0.05$, ** - $P \leq 0.01$, *** - $P \leq 0.001$, and
 962 **** - $P \leq 0.0001$. P values for % *HAC1*ⁱ and % cleavage were determined by Welch's test
 963 followed by a Games-Howell post-hoc test. ($n = 12$ for the WT, $n = 4$ for the empty vector
 964 transformed *ire1Δ* strain, and $n = 6$ for all other strains). P values for *KAR2* and *PDII*
 965 induction were obtained from an ordinary two-way ANOVA with Tukey's correction for
 966 multiple comparisons on the ln-transformed data.

967 **Figure 9. D836 is required for induction of UPRE-*lacZ* reporters by activation loop**

968 **mutants.** β -Galactosidase activity standardised to total cellular protein before, 1 h, and 2 h
 969 after induction of ER stress with 2 mM DTT in mid-exponential *ire1Δ* cells expressing the
 970 indicated *IRE1* alleles from YCplac33 or carrying empty vector ('-'). Bars represent standard
 971 errors ($n = 12$ for WT Ire1 and cells transformed with empty vector, $n = 9$ for all other

972 strains). * - $P \leq 0.05$ and **** - $P \leq 0.0001$. P values were obtained from an ordinary two-
973 way ANOVA with Tukey's correction for multiple comparisons on the ln-transformed data.

974 **Figure 10. D836 is not required for clustering of Ire1 *in vivo*.** Location of Sec63-GFP and
975 Ire1-mCherry in unstressed cells and cells exposed to 2 mM DTT for 15 min, 1 h or after
976 wash out of DTT for 1 h from cells treated with 2 mM DTT for 2 h. Sec63-GFP was
977 expressed from plasmid pJK59 in *ire1Δ* cells transformed with single copy *LEU2* plasmids
978 derived from pEvA97 that carry the indicated *IRE1* alleles. Images covering ~100 cells were
979 taken, except for the DTT wash out experiment in which ~20 cells were analysed.
980 Representative images are shown. Scale bar – 5 μm.

981 **Figure 11. Survival of ER stress by activation loop mutants requires D836.** Survival of
982 ER stress induced with 0.8 μg/ml Tm or 1.5 mM DTT. Serial 10-fold dilutions of fresh
983 overnight cultures of *ire1Δ* cells expressing the indicated *IRE1* alleles from YCplac33 or
984 carrying empty vector were spotted on SD minus uracil plates containing 0.8 μg/ml Tm or 1.5
985 mM DTT and allowed to grow for 2-3 d before taking photographs. The experiment was
986 repeated three times with qualitatively similar results.

987 **Figure 12. Mutation of phosphorylation sites in the activation does not alter inactivation**
988 **of Ire1.** (A) Northern blots for *HAC1*, *KAR2*, *PDII*, and the loading control pC4/2 (40) on
989 RNA extracted from *ire1Δ* strains expressing the indicated *IRE1* alleles from YCplac33 or
990 carrying empty vector ('-'). Mid-exponential growth phase cells were treated with 2 mM
991 DTT for 2 h, before washing the cells once with culture medium and resuspending the cells in
992 fresh, DTT-free medium. (B) Plot of the natural logarithm of the percentage of *HAC1*ⁱ mRNA
993 over time. (C) Plot of the natural logarithm of the percentage of *HAC1* mRNA splicing over
994 time. (D) Plot of the natural logarithm of *KAR2* mRNA over time. (E) Plot of the natural
995 logarithm of *PDII* mRNA over time. Dotted lines represent the 95% confidence intervals of

996 the linear regression models. The first order rate constants, k_{off} , were calculated from the
997 slopes of the linear regression models.

998 **Figure 13. Mutation of all phosphorylation sites in the activation loop of Ire1 is epistatic**
999 **to overexpression of Ptc2. (A)** Effect of overexpression of WT and catalytically inactive
1000 E37A-D38A Ptc2 from the *GALI* promoter on a 2 μ plasmid on survival of ER stress induced
1001 with 0.8 $\mu\text{g/ml}$ Tm. Fresh overnight cultures of *ire1* Δ cells expressing the indicated *IRE1*
1002 alleles from YCplac33 and the indicated *P_{GALI}-PTC2* alleles from pRSII422 were grown on
1003 1% (w/v) raffinose and 2% (w/v) galactose and spotted in 10 fold serial dilutions onto plates
1004 containing 1% (w/v) raffinose and 2% (w/v) galactose and, where indicated, 0.8 $\mu\text{g/ml}$ Tm.
1005 Plates were incubated for 7 d at 30 °C. The negative decadic logarithms of the dilutions *D* of
1006 the 10-fold dilution series are shown on top of the plates. The threshold dilutions for
1007 untreated cells, $D_{\text{T,u}}$, and cells exposed to tunicamycin, $D_{\text{T,Tm}}$, and the difference between
1008 both threshold dilutions, $\Delta\log D_{\text{T}}$, are shown to the right of the plates. **(B)** Effect of
1009 overexpression of Dcr2 by placing the *GALI* promoter in front of the endogenous *DCR2* gene
1010 on survival of ER stress. Serial 10-fold dilutions of fresh overnight cultures of *ire1* Δ cells and
1011 *ire1* Δ *P_{GALI}-T7-DCR2* cells expressing WT *IRE1* from YCplac33 grown on 1% (w/v)
1012 raffinose and 2% (w/v) galactose were spotted onto plates containing 1% (w/v) raffinose and
1013 2% (w/v) galactose and, where indicated, 0.4 $\mu\text{g/ml}$ or 0.8 $\mu\text{g/ml}$ Tm. Plates were incubated
1014 for 4 d at 30 °C. **(C)** Effect of overexpression of WT and catalytically inactive H338A Dcr2
1015 from the *GALI* promoter on a 2 μ plasmid on survival of ER stress. Fresh overnight cultures
1016 of *ire1* Δ cells expressing the indicated *IRE1* alleles from YCplac33 and the indicated *P_{GALI}-*
1017 *DCR2* alleles from pRSII422 were grown on 1% (w/v) raffinose and 2% (w/v) galactose and
1018 spotted in 10 fold serial dilutions onto plates containing 1% (w/v) raffinose and 2% (w/v)
1019 galactose and, where indicated, 0.4 $\mu\text{g/ml}$ Tm. Plates were incubated for 7 d at 30 °C. **(D)**
1020 Deletion of both *DCR2* and *PTC2* does not affect survival of ER. Serial 10-fold dilutions of

1021 fresh overnight cultures of *ire1Δ* cells, *ire1Δ dcr2Δ* cells, *ire1Δ ptc2Δ* cells, and *ire1Δ dcr2Δ*
1022 *ptc2Δ* cells expressing the indicated *IRE1* alleles from YCplac33 were spotted onto SD minus
1023 uracil plates containing 0.4 μg/ml Tm, 1 mM DTT, or 2 mM 2-deoxy-D-glucose (2-DOG) to
1024 induce ER stress. Plates were incubated for 3 d at 30 °C. All spotting assays were repeated at
1025 least once with qualitatively similar results.
1026

1027 **Table 1.** Oligodeoxynucleotides. Restriction sites are underlined. Mutagenic base
 1028 substitutions in oligodeoxynucleotides used for site-directed mutagenesis are shown in bold.

Name	Sequence
8691G	TGTGCAGGAT <u>CCCAA</u> AGATTCAAATTTTGCCGCC
DCR2-H338A-F	CAATGGTATGGGGAAAT GCC GACGACGAGGGAAGCT
DCR2-H338A-R	AGCTTCCCTCGTCGTCG GC ATTTCCCCATACCATTG
H4075A04	TGCCTTAGAACTTTCATAGC
H8293	GGTCTTTGCAAAAACTAGAC <u>GCCGGC</u> CAGGCAGCATTTAGAGCAA AT
H8294	ATTTGCTCTAAATGCTGCCTG <u>GCCGGC</u> GTCTAGTTTTTTTGCAAAGA CC
H8623	TTGATATCAGACTTTGGTCTTTGCAAAAACTAG <u>CTAGC</u> GGTCAGT CTTCATTTAGAACAAATTTGAATAACC
H8624	GGTTATTCAAATTTGTTCTAAATGAAGACTGACC <u>GCTAGC</u> TAGTTT TTTGCAAAGACCAAAGTCTGATATCAA
H8625	TTTGATATCAGACTTTGGTCTTTGCAAAAACTAG <u>CTAGC</u> GGTCAG GCTGCATTTAGAACAAATTTG
H8626	CAAATTTGTTCTAAATGCAGCCTGACC <u>GCTAGC</u> TAGTTTTTTTGCAA AGACCAAAGTCTGATATCAA
H8627	ATCAGACTTTGGTCTTTGCAAAAACTAG <u>CTAGC</u> GGTCAGGCAGCA TTTAGAGCAAATTTGAATAACCCTGCA
H8628	GGTTATTCAAATTTGCTCTAAATGCTGCCTGACC <u>GCTAGC</u> TAGTT TTTTGCAAAGACCAAAGTCTGAT
H8629	ATCAGACTTTGGTCTTTGCAAAAA <u>GCTAGC</u> CGCCGGCCAGGCAGCA TTTAGAGCAAATTTGAATAACCCTGCA

H8630 GGGTTATTCAAATTTGCTCTAAATGCTGCCTGGCCGGCGGCTAGCT
TTTTGCAAAGACCAAAGTCTGAT

H9327 TCATAAATACGGATACGTCTTTCTGTACCTCCATAGCCAGCATAAC
CACCAAGCTTCGTACGCTGCAGG

H9328 AGTTTTATACTTAAGTATCGAAGACCAGCACCGTGGTTAAAAATCT
TAACAGGCCACTAGTGGATCTG

H9329 GCCGGAGGTCTTGCTCTTGGATTGGCTGGAAGGGTCAAGATTTTCT
GCATAAGCTTCGTACGCTGCAGG

H9330 TCCCTAGGATTTTGACTATTCCATTGTTGTATAAAAATATAGAGAAC
CAGAAGGCCACTAGTGGATCTG

H9331 ACTACCAAGTATAATAGGTACCTTTGATACAGCCTCGGTAACCGGA
TCATAACCATTGCTGTCCACCAG

H9332 CCGGAGTGGCTCTCTTTATCAATTACCGGGTTTGATAGAATTTGTC
CCATAACCATTGCTGTCCACCAG

PTC2-E37A-D38A-F ACATTAGGCTCTAGAATGTGTGAAGCCGCCATGGACATCCGCCACC

PTC2-E37A-D38A-R GGTGGCGGATGTCCATGGCGGCTTCACACATTCTAGAGCCTAATGT

U5803H01 TAAATGGCTAGCATGACTGGTGGACAGCAAATGGGTG

U5803H02 GATCCACCCATTGCTGTCCACCAGTCATGCTAGCCATTTAAT

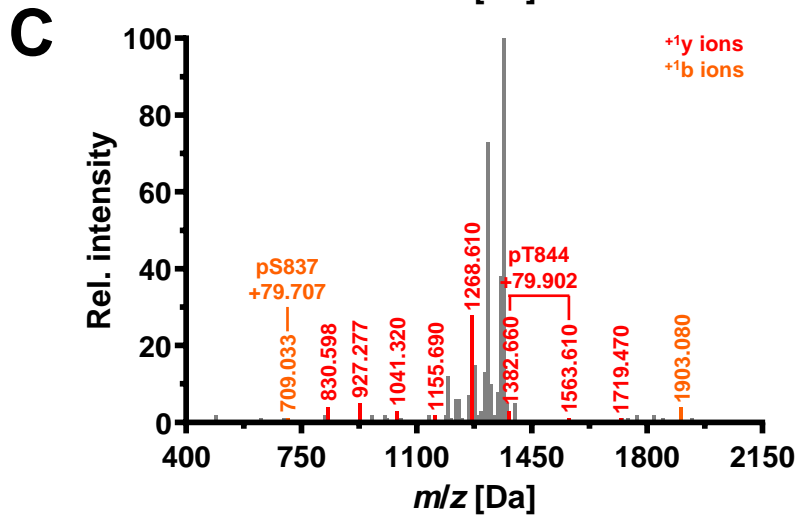
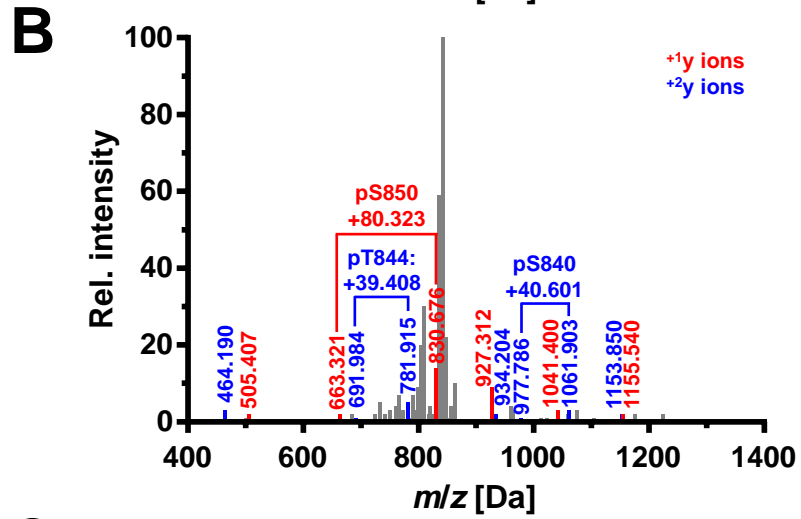
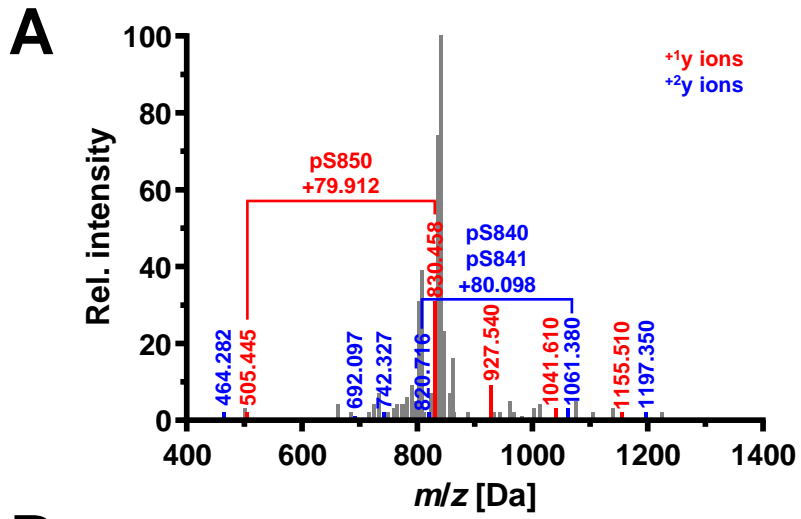
1030 **Table 2.** *Saccharomyces cerevisiae* strains. All strains, except Y01907, carry the alleles
 1031 *MATa ade2-1 can1-100 his3-11,-15 leu2-3,-112 trp1-1 ura3-1*.

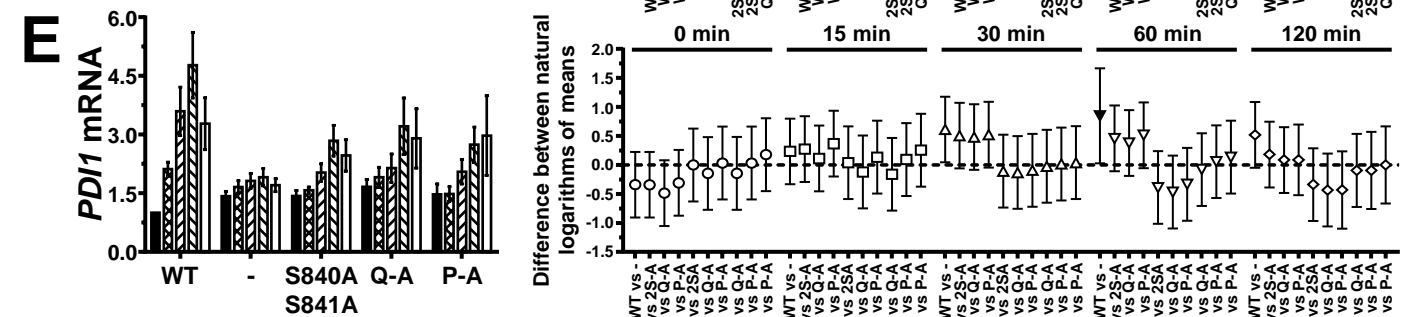
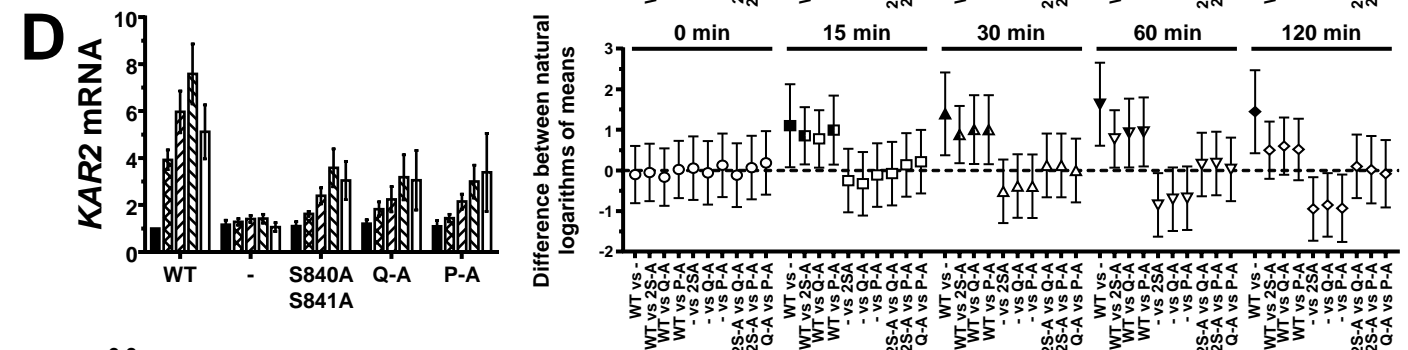
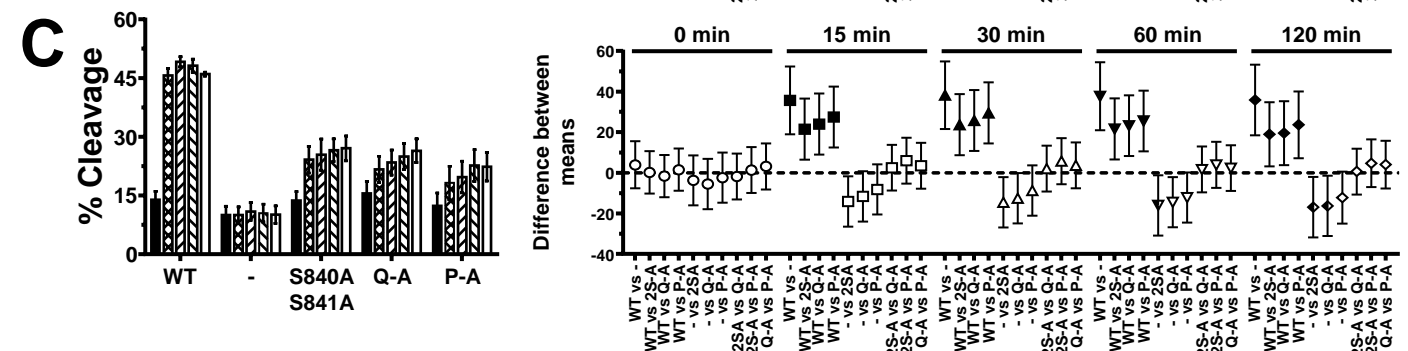
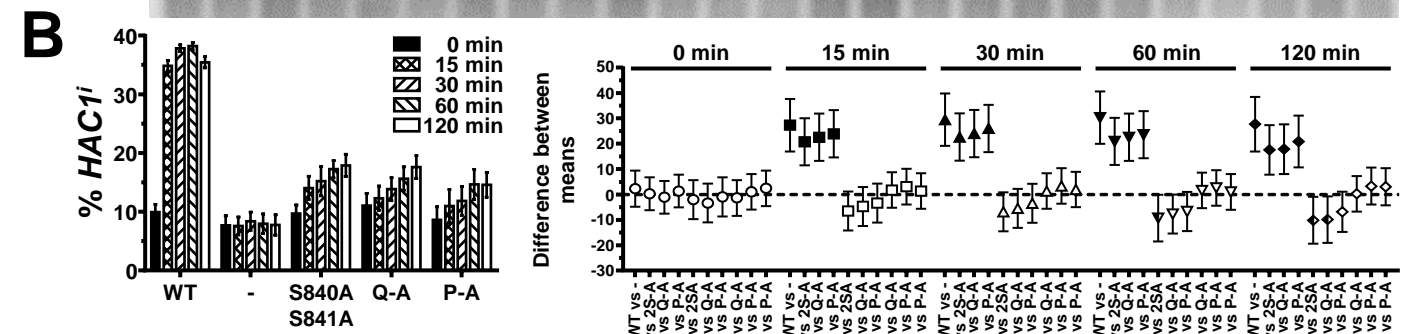
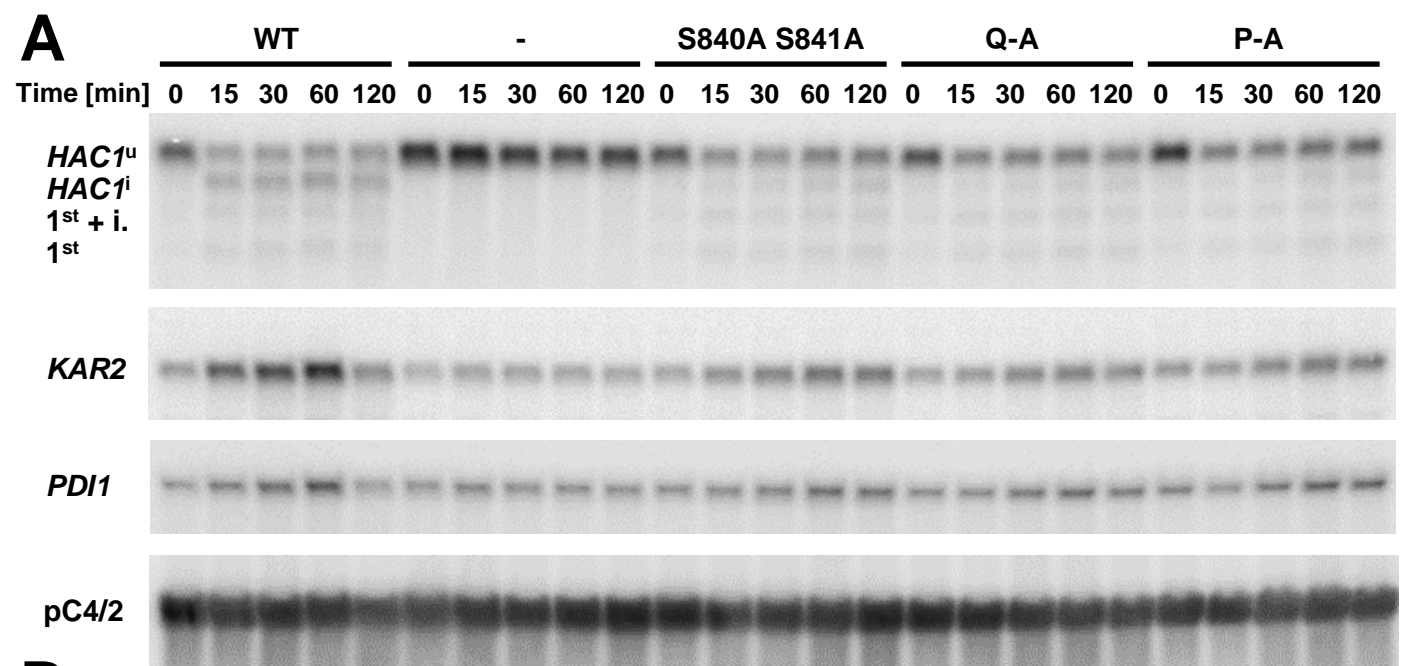
Name	Genotype	Reference
W303-1A		(33)
PWY 260	<i>ire1Δ::TRP1 his3-11,15::HIS3⁺UPRE-lacZ leu2-3,-112::LEU2⁺UPRE-lacZ</i>	(23)
MSY 14-02	<i>ire1Δ::kanMX2</i>	This study.
MSY 792-02	<i>ire1Δ::TRP1 dcr2Δ::kanMX2 his3-11,15::HIS3⁺UPRE-lacZ leu2-3,-112::LEU2⁺UPRE-lacZ</i>	This study.
MSY 793-06	<i>ire1Δ::TRP1 ptc2Δ::kanMX2 his3-11,15::HIS3⁺UPRE-lacZ leu2-3,-112::LEU2⁺UPRE-lacZ</i>	This study.
MSY 794-11	<i>ire1Δ::TRP1 kanMX6-P_{GALI,10}-T7-DCR2 his3-11,15::HIS3⁺UPRE-lacZ leu2-3,-112::LEU2⁺UPRE-lacZ</i>	This study.
MSY 795-01	<i>ire1Δ::TRP1 kanMX6-P_{GALI,10}-T7-PTC2 his3-11,15::HIS3⁺UPRE-lacZ leu2-3,-112::LEU2⁺UPRE-lacZ</i>	This study.
MSY 796-02	<i>ire1Δ::TRP1 dcr2Δ::kanMX2 ptc2Δ::hphNT1 his3-11,15::HIS3⁺UPRE-lacZ leu2-3,-112::LEU2⁺UPRE-lacZ</i>	This study.
MSY 797-02	<i>ire1Δ::TRP1 dcr2Δ::hphNT1 ptc2Δ::kanMX2 his3-11,15::HIS3⁺UPRE-lacZ leu2-3,-112::LEU2⁺UPRE-lacZ</i>	This study.
Y01907	<i>MATa his3Δ1 leu2Δ0 met15Δ0 ura3Δ0 ire1Δ::kanMX4</i>	(70)

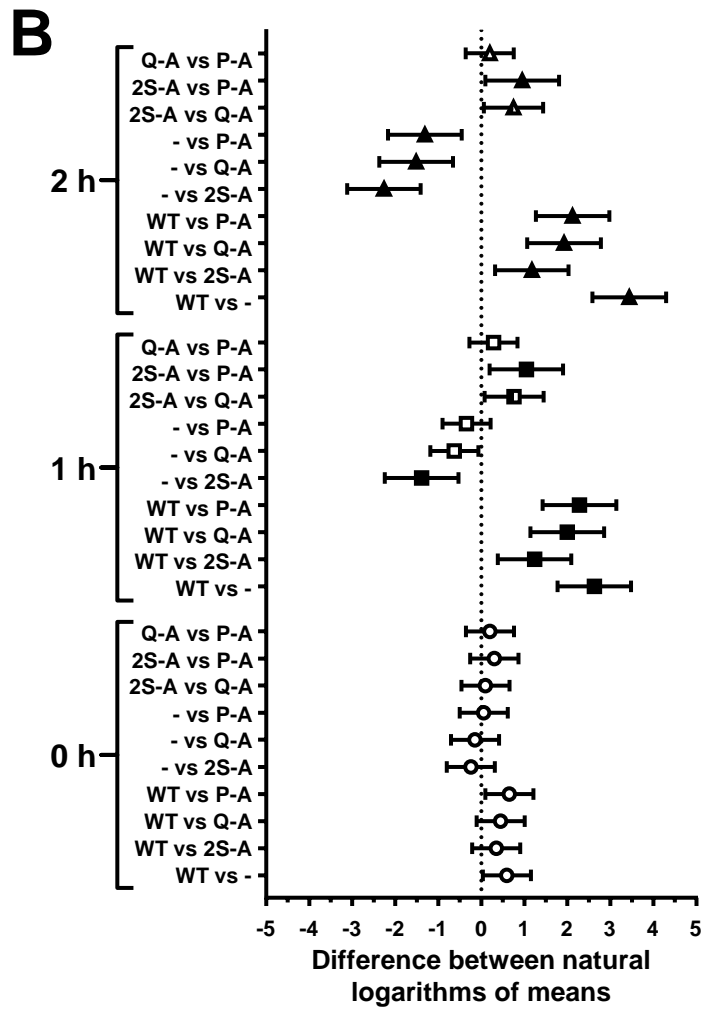
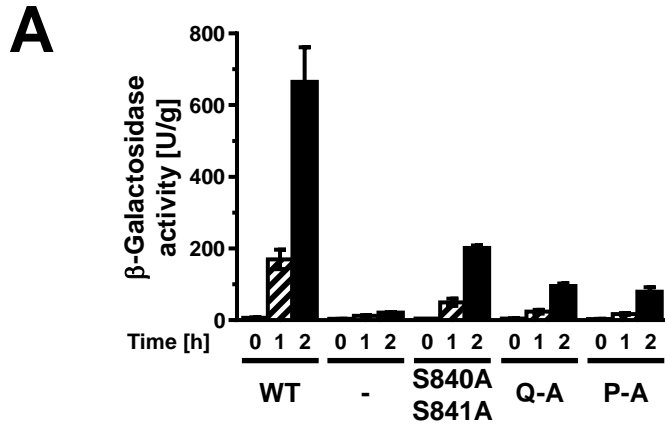
1032

1033

		P-A mutant			
		Q-A mutant			
		A	AA	A	A
		↑	↑↑	↑	↑
<i>S. cerevisiae</i>	828	DFGLCKK	LD-SG-QSSF-RT-NLNN	PS-GTSGWRAPE	859
<i>S. bayanus</i>	828	DFGLCKK	LD-SG-QSSF-RT-NLNN	PS-GTSGWRAPE	859
<i>A. fumigatus</i>	858	DFGLCKK	LD-D-NQSSFRAT--TAH	AA-GTSGWRAPE	889
<i>A. gossypii</i>	843	DFGLCKK	LEAE--ESSF-KT-NINN	AA-GTSGWRAPE	874
<i>C. albicans</i>	928	DFGLCKK	LEND--QSSFRAT--TQN	AASGTSGWRAPE	960
<i>T. reesei</i>	953	DFGLCKK	LE-D-RQSSFGAT--TGR	AA-GTSGWRAPE	984
<i>C. elegans</i>	659	DFGLCKR	VQP-GKNS-ISRGIASG-	LA-GTDGWIAPE	691
<i>D. melanogaster</i>	690	DFGLCKK	LNF-GKTS-FSRR--SG-	VT-GTDGWIAPE	720
<i>H. sapiens</i> alpha	711	DFGLCKK	LAV-GRHS-FSRR--SG-	VP-GTEGWIAPE	741
<i>H. sapiens</i> beta	660	DFGLCKK	LPA-GRCS-FSLH--SG-	IP-GTEGWMIAPE	690
<i>A. thaliana</i> 1	628	DMGISKR	LPAD--TSA-KTRNST-	GLGGSSGWQAPE	660
<i>A. thaliana</i> 2	590	DMGISKR	MSRD--MSSLGH--LAT-	GS-GSSGWQAPE	620
		Mg ²⁺ β10	Activation loop	P+1 loop	

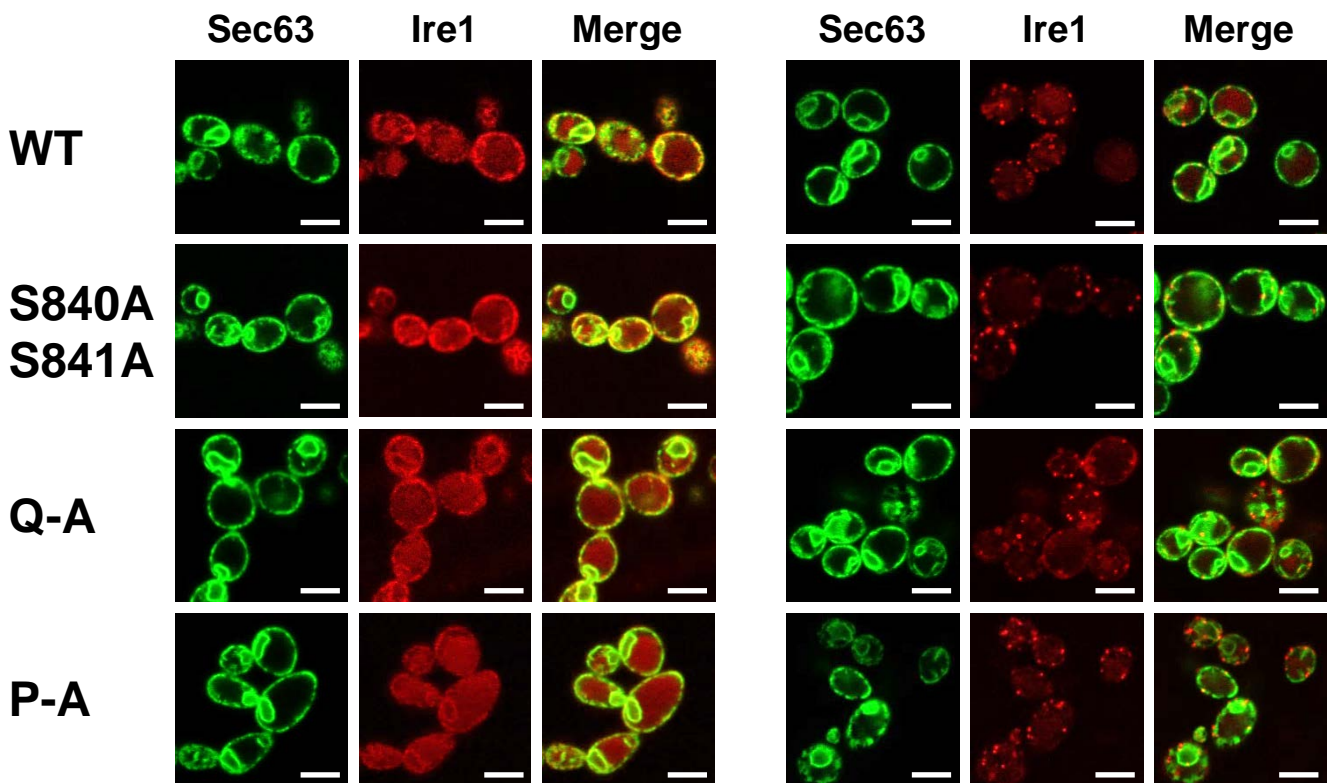






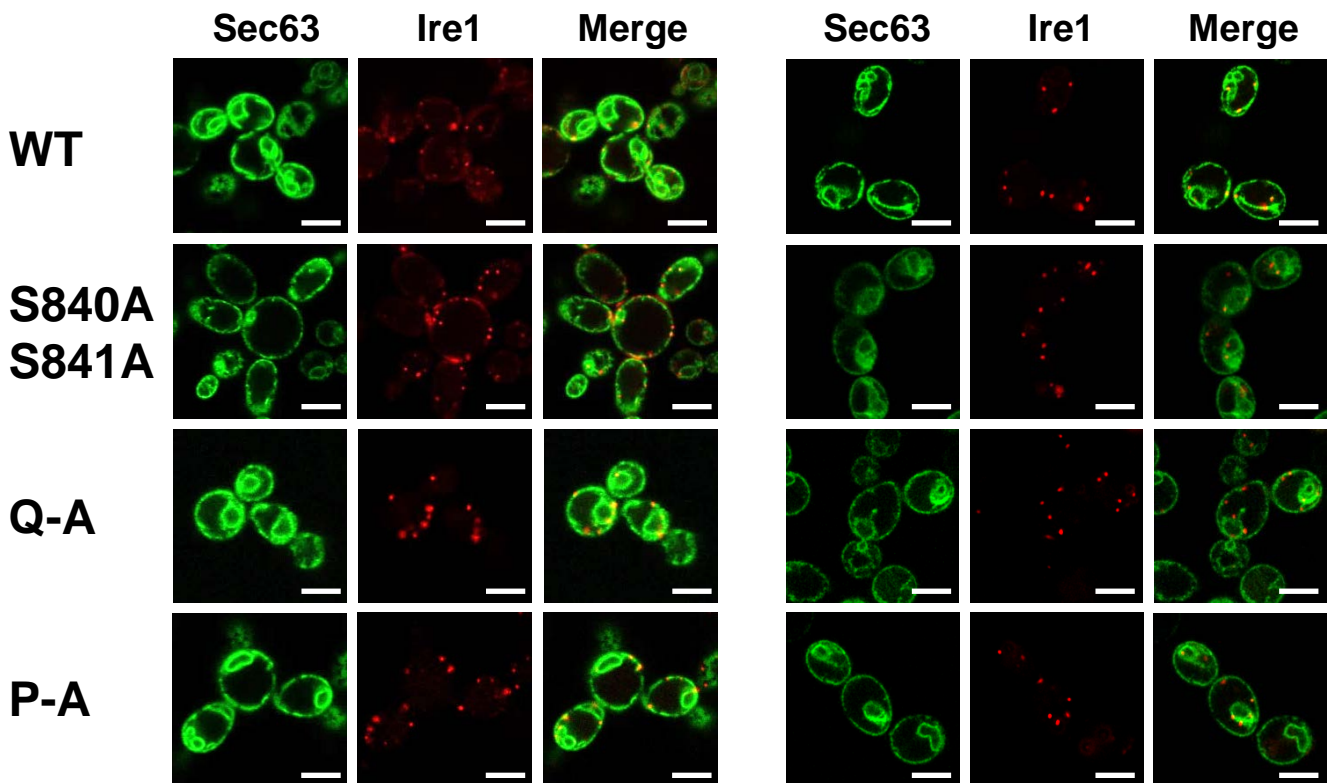
- DTT

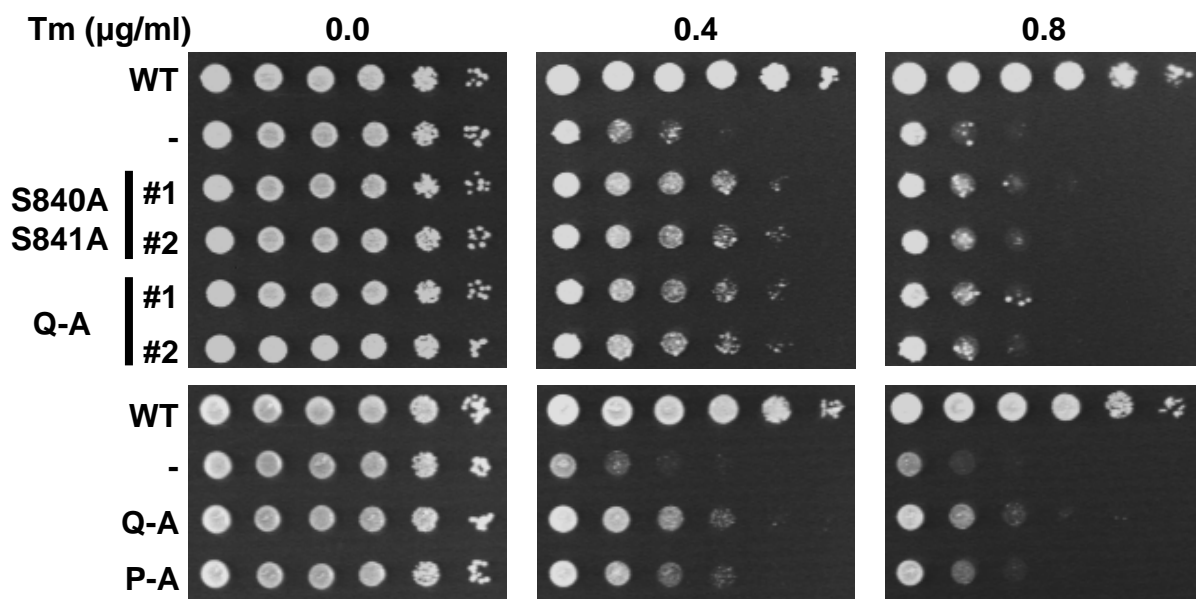
+ 2 mM DTT 15 min

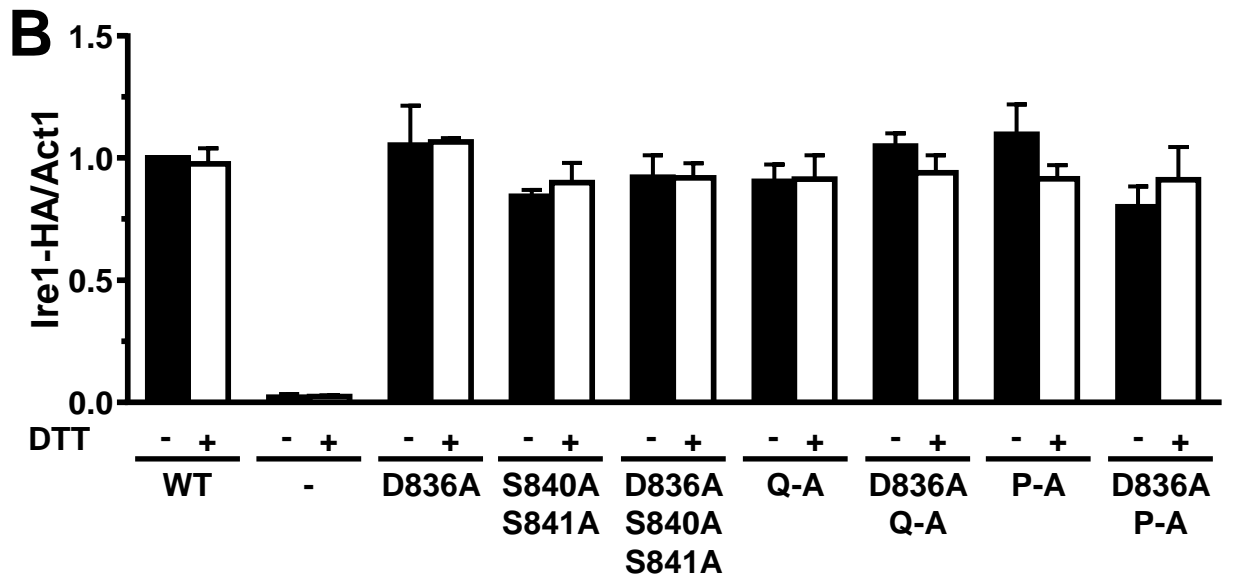
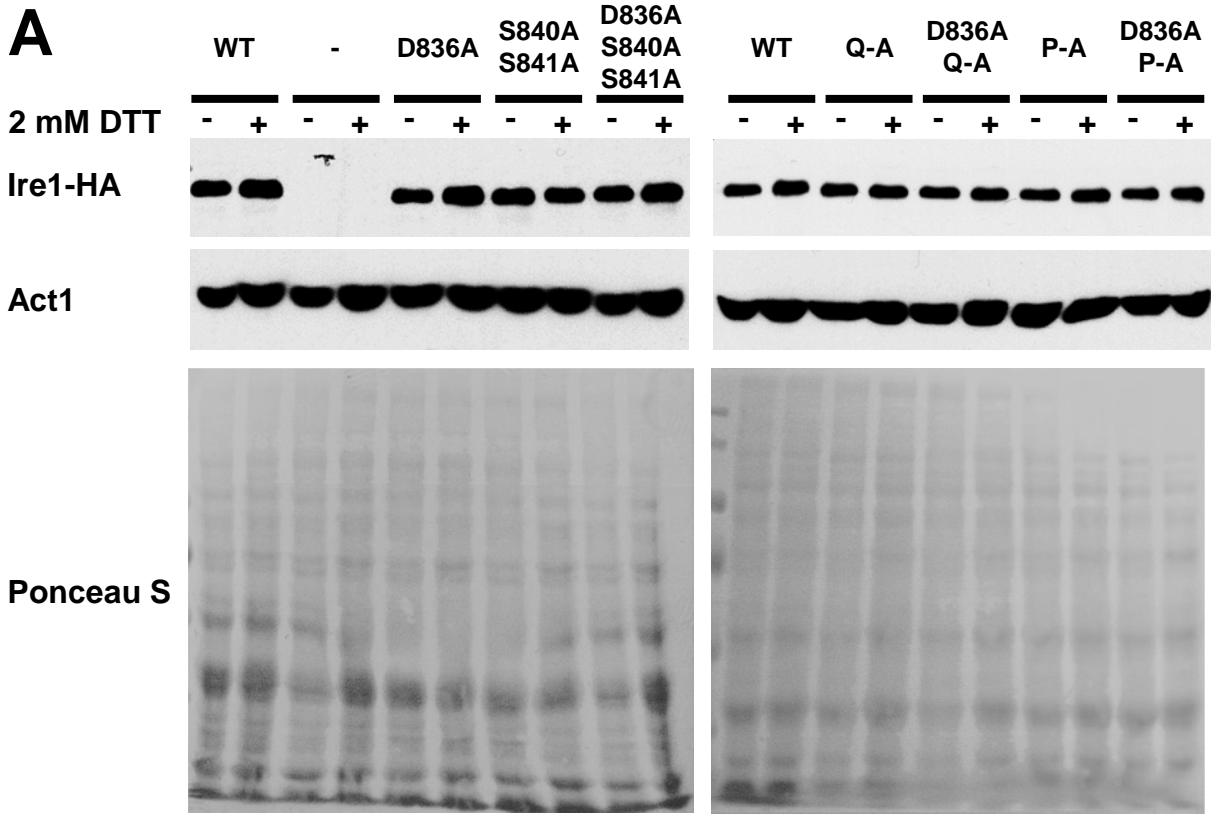


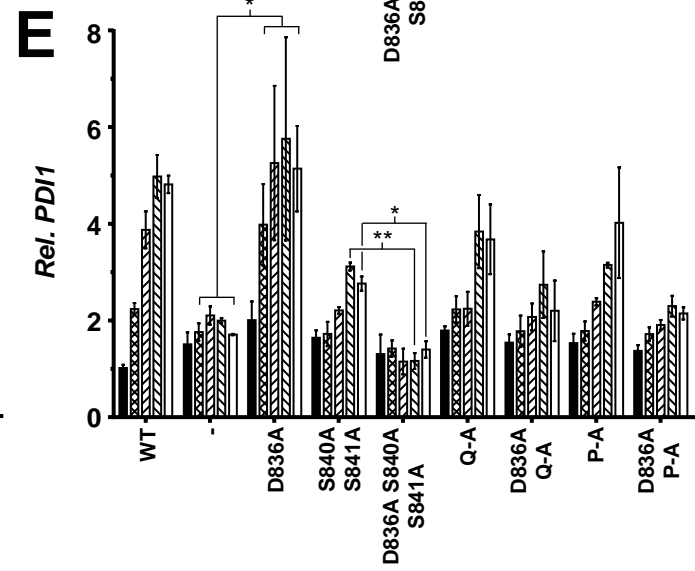
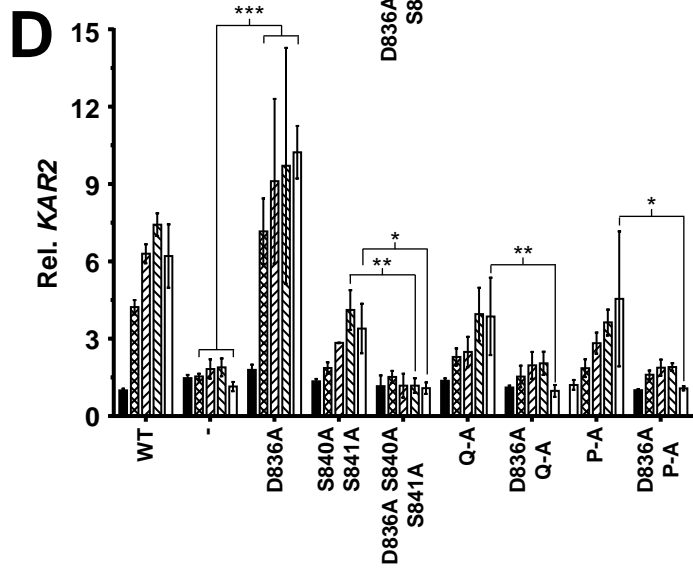
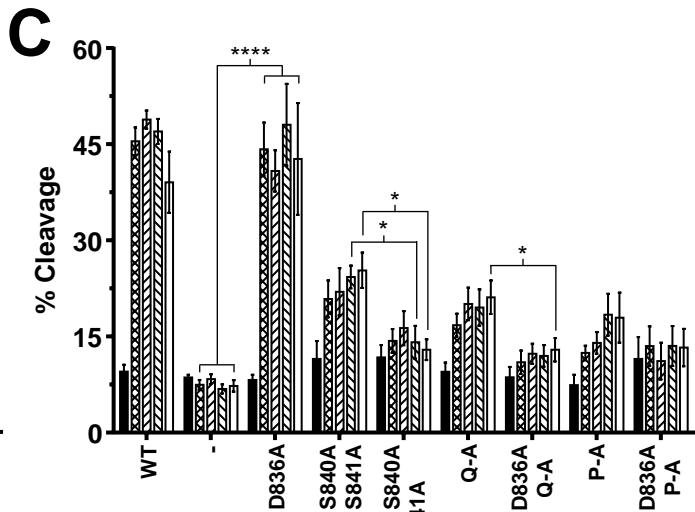
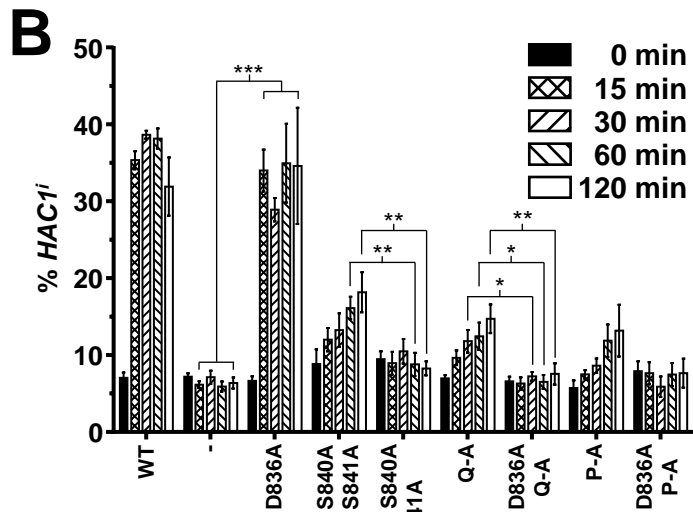
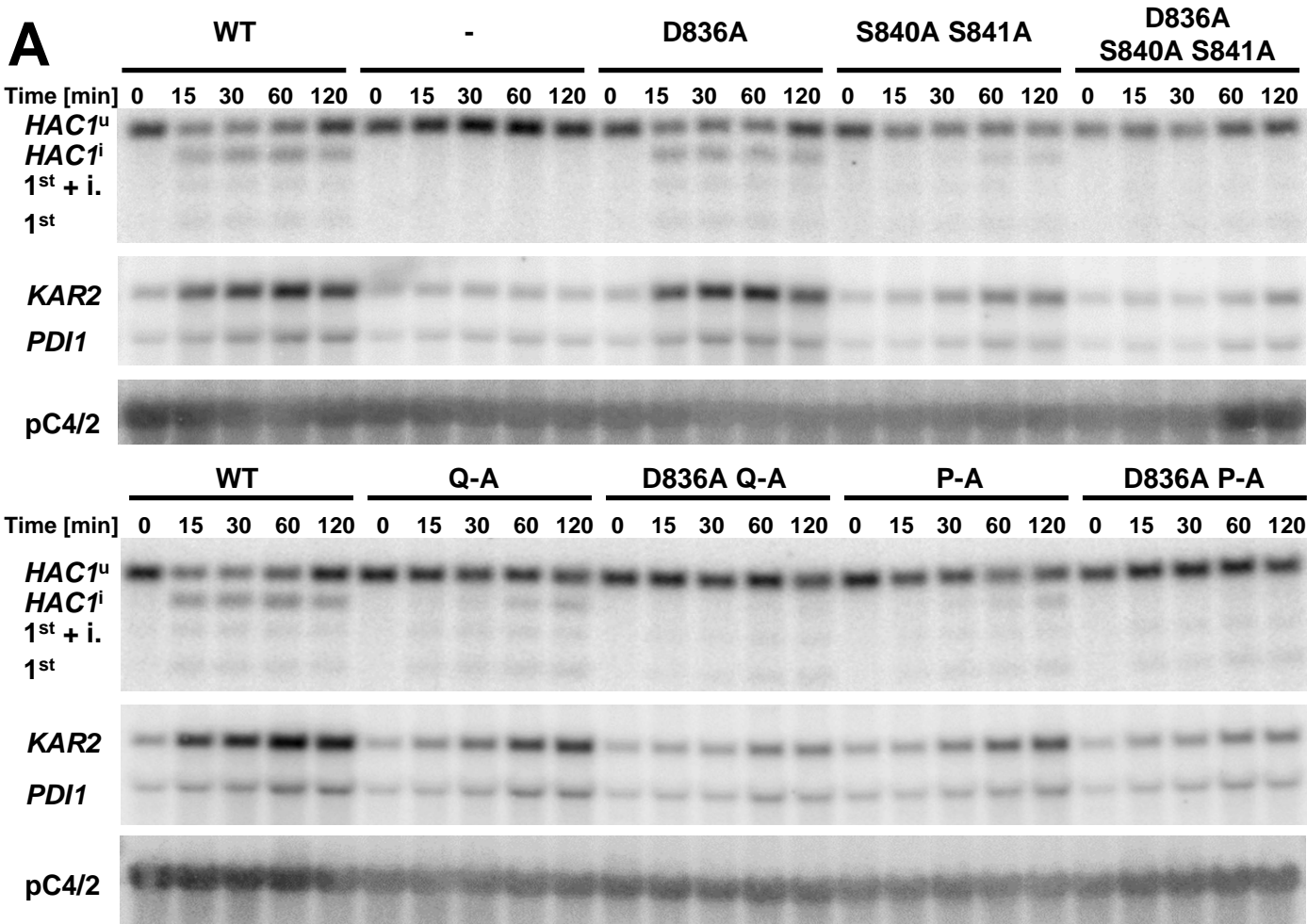
+ 2 mM DTT 60 min

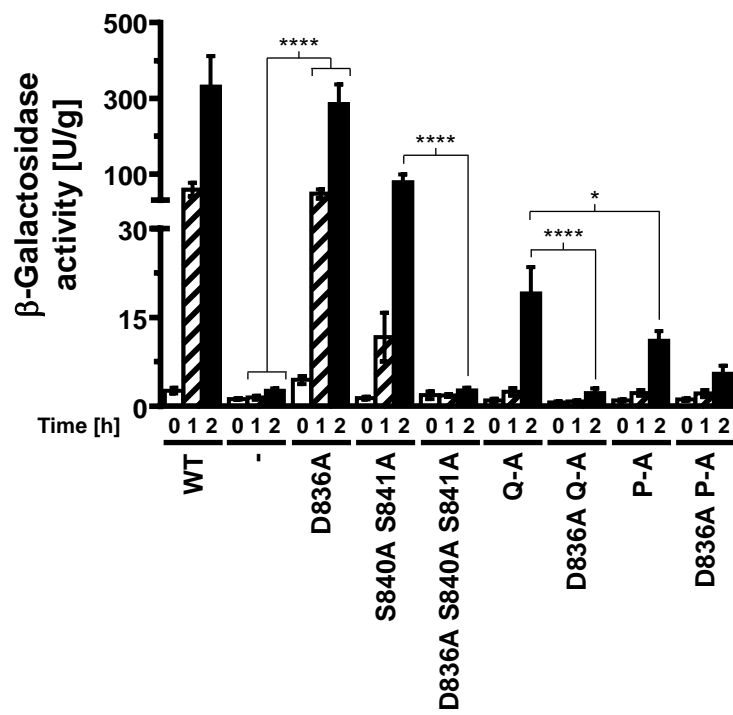
60 min after 2 mM DTT

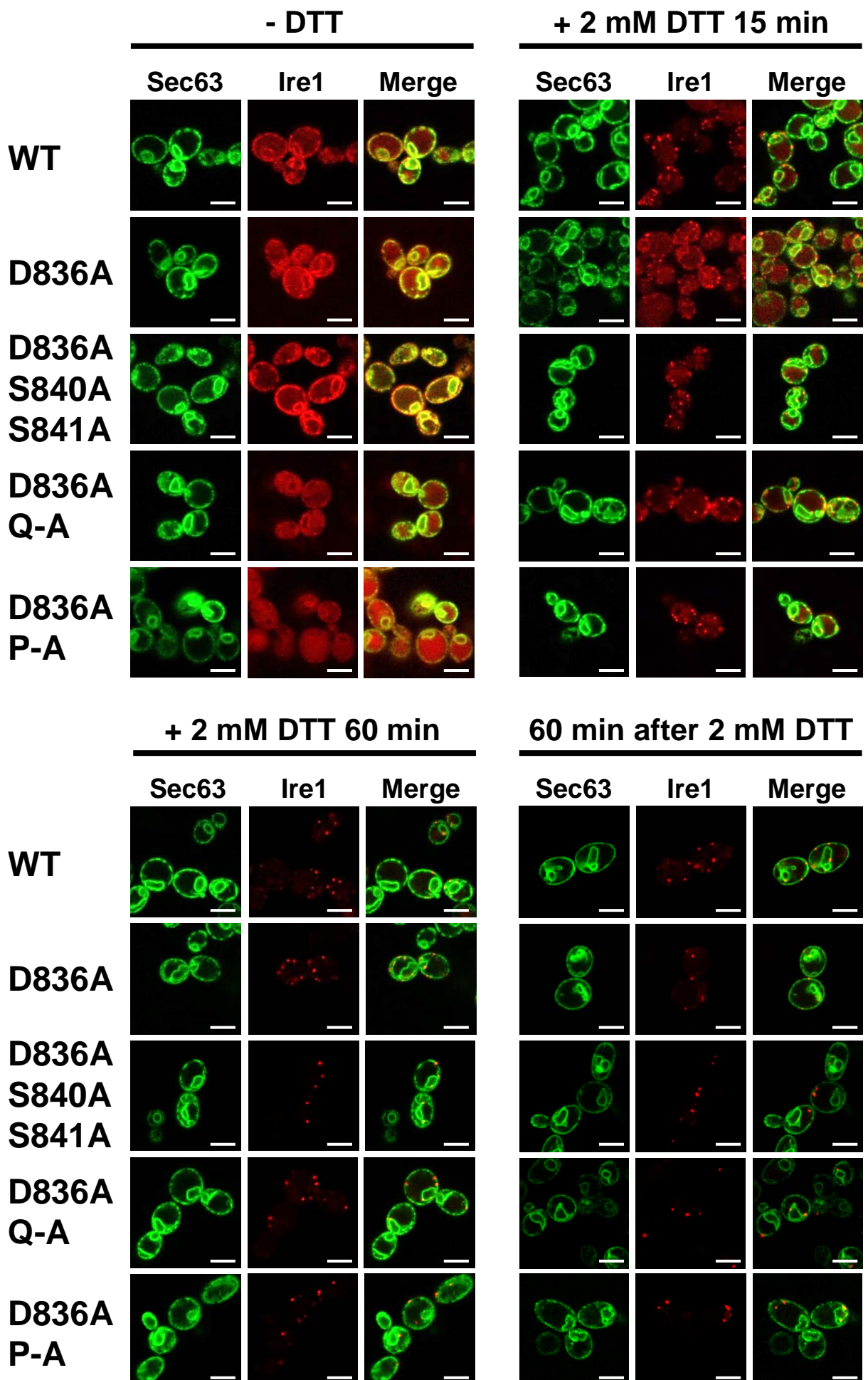












Untreated

0.8 μ g/ml Tm

1.5 mM DTT

WT



D836A



S840A S841A



D836A S840A S841A



Q-A



D836A Q-A



WT



D836A



P-A



D836A P-A



WT



D836A



S840A S841A



D836A S840A S841A



Q-A



D836A Q-A



WT



D836A



P-A



D836A P-A

